THE JOURNAL OF BIOLOGICAL CHEMISTRY VOL. 284, NO. 6, pp. 3513–3520, February 6, 2009

A Single Amino Acid of Toll-like Receptor 4 That Is Pivotal for Its Signal Transduction and Subcellular Localization*

Received for publication, April 22, 2008, and in revised form, October 29, 2008 Published, JBC Papers in Press, December 8, 2008, DOI 10.1074/jbc.M803086200

Shintaro Yanagimoto[‡§¶], Keita Tatsuno[§], Shu Okugawa[§], Takatoshi Kitazawa[§], Kunihisa Tsukada[§], Kazuhiko Koike[§], Tatsuhiko Kodama[¶], Satoshi Kimura[‖], Yoshikazu Shibasaki[‡1], and Yasuo Ota[1,2]**

From the [‡]Center for Structuring Life Sciences, Graduate school of Arts and Sciences, University of Tokyo, Meguro-ku, Tokyo 153-8903, the [§]Department of Infectious Diseases, Graduate School of Medicine, University of Tokyo, Bunkyo-ku, Tokyo 113-8655, the [¶]Laboratory for Systems Biology and Medicine, Research Center for Advanced Science and Technology, University of Tokyo, Meguro-ku, Tokyo 153-8904, the [‖]Tokyo Teishin Hospital, Fujimi, Chiyoda-ku, Tokyo 102-8798, and the [**]Department of Medicine, Teikyo University School of Medicine, 2-11-1, Kaga, Itabashi-ku, Tokyo 173-8605, Japan

Toll-like receptor 4 (TLR4) is essential for recognizing a Gram-negative bacterial component, lipopolysaccharide (LPS). A single amino acid mutation at position 712 of murine TLR4 leads to hyporesponsiveness to LPS. In this study we determined that an amino acid, a leucine at position 815 of human TLR4, is also pivotal for LPS responsiveness and subcellular distribution. By replacing the leucine with alanine, the mutant TLR4 lost responsiveness to LPS and did not localize on the plasma membrane. In addition, it does not coprecipitate with myeloid differentiation-2, an accessory protein that is necessary for TLR4 to recognize LPS. These results suggest that the leucine at position 815 is required for the normal maturation of TLR4 and for formation of the TLR4·MD-2 complex.

Toll-like receptors (TLRs)[3] play essential roles in both innate and adaptive immunity (1). Thirteen members of the TLR family have been identified in mammals. TLRs have leucine-rich-repeats in their extracellular domains and a Toll/Interleukin-1 receptor (TIR) in their cytoplasmic domains, the latter of which mainly mediates intracellular signaling. Signaling pathways of TLRs, except for TLR3, depend on an adapter protein, MyD88 (myeloid differentiation factor 88), which interacts with the TIR domain of TLRs. This pathway leads to the activation of the transcription factor NF-κB and production of cytokines such as tumor necrosis factor-α and interleukin-6. Another important signaling pathway mediated by TLR3 and TLR4 that exploits the TIR domain is the MyD88-independent pathway. This pathway involves different adapter proteins, such as the TIR domain-containing adaptor inducing interferon-β (TRIF) and TRIF-related adaptor molecule (2–4), and is essential for production of type I interferon through activation of interferon regulatory factor-3.

TLRs recognize as ligands several microbial pathogen-associated molecular patterns. One such pathogen-associated molecular pattern is lipopolysaccharide (LPS), which is recognized by TLR4. LPS triggers severe immunologic reactions by the host in Gram-negative bacterial infections and has drawn attention in many clinical situations. TLR4 is the first mammalian TLR to be discovered in the context of immunology. TLR4 was identified in the search for the genes responsible for LPS hyporesponsiveness (5, 6). The defect was found to stem from a single amino acid mutation, replacement of proline with histidine at position 712, in the cytoplasmic tail of murine TLR4. The study led to the discovery of the importance of TLR4 in innate immunity.

A variety of cells are activated by LPS stimulation through TLR4. TLR4 forms a receptor complex with an accessory protein, myeloid differentiation-2 (MD-2). MD-2 first associates with TLR4 in the endoplasmic reticulum (ER) and *cis*-Golgi, and both proteins move together to the plasma membrane (7, 8). Upon recognition of LPS, the TLR4·MD-2 complex receives LPS on the cell surface and initiates intracellular signaling. The expression of TLR4 in the absence of MD-2 does not confer full responsiveness to LPS stimuli in experimental cell lines (9). An analysis of MD-2 knockout mice revealed that MD-2 is important not only for LPS sensing but also for cellular distribution of TLR4.

In this study we hypothesized that the cytoplasmic tail of TLR4 contains regions that control both localization and signaling. Using truncation and mutation analysis, and paying particular attention to the TIR domain, we identified a single amino acid that is pivotal for both TLR4 signaling and subcellular distribution. The site we found was on the C-terminal portion of the TIR domain for which no specific function has been yet determined.

* This work was partly supported by the Program of Fundamental Studies in Health Sciences of the National Institute of Biomedical Innovation, by the Focus 21 project of the New Energy and Industrial Technology Development Organization, and by the Special Coordination Fund for Science and Technology from the Ministry of Education, Culture, Sports, Science and Technology. This study was also partly supported by a grant-in-aid from the Ministry of Education, Culture, Sports, Science and Technology (to Y. O.). The costs of publication of this article were defrayed in part by the payment of page charges. This article must therefore be hereby marked "*advertisement*" in accordance with 18 U.S.C. Section 1734 solely to indicate this fact.

[1] Both authors contributed equally to this work.

[2] To whom correspondence should be addressed. Tel.: 81-3-3964-1211 (ext. 1756); Fax: 81-3-3579-6310; E-mail: yasuota-tky@umin.ac.jp.

[3] The abbreviations used are: TLR, Toll-like receptor; TIR, Toll/Interleukin-1 receptor; TRIF, TIR domain-containing adaptor inducing interferon-β; LPS, lipopolysaccharide; MD-2, myeloid differentiation-2; ER, endoplasmic reticulum; GFP, green fluorescent protein; EGFP, enhanced GFP; RLA, relative luciferase activity; Sulfo-NHS-SS-Biotin, sulfosuccinimidyl-2-(biotinamido)ethyl-1,3-dithiopropionate.

EXPERIMENTAL PROCEDURES

Reagents and Other Materials—Lipopolysaccharide (LPS) from *Escherichia coli* O55:B5 was purchased from Sigma-Aldrich and applied without repurification. FLAG- and hexa-histidine (His_6)-tagged human TLR4 expression plasmid (pEFBOS/humanTLR4flaghis) and FLAG- and His_6-tagged human MD-2 expression plasmid (pEFBOS/humanMD-2flaghis) were generous gifts from Dr. Kensuke Miyake (Institute of Medical Science, University of Tokyo, Japan). Human CD14 cDNA plasmid (pCMV6-XL5/humanCD14) was purchased from OriGene (Rockville, MD). Fluorescent protein expression vector pEGFP-N3 was purchased from Clontech (Mountain View, CA). Anti-TLR4 monoclonal antibody (clone HTA125) was purchased from Abcam (Cambridge, MA). Anti-FLAG monoclonal antibody (clone M2) was purchased from Sigma-Aldrich. Anti-*A.v.* (GFP) monoclonal and polyclonal antibodies were purchased from Clontech. Control immunoglobulins for immunoprecipitation were purchased from BD Biosciences (San Jose, CA). Horseradish peroxidase-labeled anti-immunoglobulins antibodies were purchased from Dako (Glostrup, Denmark). BlockAce (DS Pharma Biomedical, Osaka, Japan) solution was used as blocking buffer for Western blotting.

Cell Culture—Human embryonic kidney (HEK) 293T cells were maintained in Dulbecco's modified Eagle's medium (Sigma-Aldrich) containing 10% heat-inactivated fetal bovine serum supplemented with penicillin-streptomycin solution (Invitrogen). FuGENE 6 transfection reagent (Roche Applied Science) was used for transient cotransfection according to the manufacturer's instructions. Culture dishes or plates were prepared to 70% confluence prior to transfection. Cells were used for experiments 36 h later. The transfection conditions were optimized for microscopic observation of the expressed fluorescent protein and were kept unchanged in other experiments.

Expression Vector Subcloning and Mutagenesis—Wild-type TLR4 cDNA was excised from pEFBOS/humanTLR4flaghis and subcloned into pEGFP-N3 so that when expressed enhanced green fluorescent protein (EGFP) would be fused at the C terminus of TLR4 (pEGFP-N3/humanTLR4). All mutations were introduced into pEFBOS/humanTLR4flaghis and pEGFP-N3/humanTLR4 using the QuikChange site-Directed mutagenesis kit (Stratagene, La Jolla, CA) according to the manufacturer's instructions and were confirmed by sequencing. For the truncation analysis, two identical unique restriction sites were prepared in the TLR4-coding region of pEFBOS/humanTLR4 using a QuikChange kit, and the DNA fragment to be removed, which was a part of the C terminus of TLR4, was excised enzymatically. After agarose gel purification, the linear double-stranded DNA was ligated to re-form a circular plasmid. Restriction sites were designed so as not to cause a frameshift between TLR4 and EGFP.

Confocal Laser Scanning Microscopy of Cells—Samples were fixed in 3% paraformaldehyde-phosphate-buffered saline at 37 °C for 10 min. Fluorescence images of fixed samples were recorded using a FluoView FV1000 Confocal Microscope (an inverted confocal laser scanning microscope, Olympus, Tokyo, Japan).

Immunoprecipitation—Transfected cells were lysed in lysis buffer (50 mM Tris-HCl, pH 7.5, 100 mM NaCl, 0.1% Triton X-100, 1 mM 1,4-dithiothreitol, and proteinase inhibitor mixture), sonicated, and centrifuged at 4 °C. Antibody was added to the supernatant, and the sample was rotated 1 h at 4 °C followed by the addition of protein G-Sepharose (GE Healthcare Life Sciences, Piscataway, NJ) and an additional 8-h incubation at 4 °C. Bound protein was washed three times in lysis buffer. Proteins were eluted by boiling in SDS sample buffer.

Biotinylation and Purification of Cell Surface Proteins—Prior to surface biotinylation, HEK 293T cells plated in a 100-mm dish were transiently transfected as described above. Surface biotinylation and subsequent purification of biotinylated proteins were performed using a Cell Surface Protein Biotinylation and Purification Kit (Pierce) following the manufacturer's instructions. Briefly, membrane-impermeable sulfosuccinimidyl-2-(biotinamido)ethyl-1,3-dithiopropionate (Sulfo-NHS-SS-Biotin) was added to cell monolayers in the culture dishes and covalently bound to amines in proteins exposed on the cell surface. The affinity resin that binds to the biotin end of Sulfo-NHS-SS-Biotin was used to collect the biotinylated proteins. Reduction by 1,4-dithiothreitol causes cleavage of the disulfide bond in Sulfo-NHS-SS-Biotin, and the elute contains the biotinylated cell surface proteins. Each final sample obtained was considered to contain proteins from an equal amount of cells, because all culture plates were treated equally and grown to full confluence. All samples were sonicated and subjected to SDS-PAGE and Western blotting. The membrane to which protein was transferred was blocked in blocking buffer for 1 h. Then the membrane was incubated with a primary antibody, followed by incubation with horseradish peroxidase-labeled anti-immunoglobulins antibody. The protein bands were then visualized by using a chemiluminescence reagent, Immobilon Western Chemiluminescent HRP Substrate (Millipore, Billerica, MA), according to the manufacturer's instructions.

Cell Stimulation Assays—HEK293T cells were plated and transiently transfected for assays. Thirty-six hours after the transfection, LPS was added to fresh culture medium in each well of the culture plates at the stated concentration. The duration of LPS stimulation was 7 h.

Dual Luciferase Reporter Assays for NF-κB Activation—HEK293T cells were plated in 12-well culture plates (4×10^4 cells/well), and experimental cDNA plasmids were transiently transfected 36 h later using the FuGENE 6 transfection reagent with 0.5 μg of NF-κB reporter plasmid expressing firefly luciferase (pNF-κB-Luc, Stratagene) and 0.05 μg of constitutively active *Renilla* luciferase reporter plasmid (pRL-TK, Promega, Madison, WI) in addition to 0.5 μg each of TLR4-EGFP plasmid and MD-2 plasmid. Stimulation experiments were performed 36 h later. Firefly luciferase and *Renilla* luciferase activities were measured using the Dual-Luciferase Reporter Assay System (Promega) and the Genelight55 luminometer (Microtech, Chiba, Japan). Relative luciferase activity (RLA) was obtained as the ratio of firefly luciferase activity to *Renilla* luciferase activity. Results are expressed as the ratio of RLA with LPS stimulation to RLA without LPS stimulation ([RLA LPS+]/[RLA LPS−]). This ratio should ideally approach 1 when no response to LPS stimulation is observed.

FIGURE 1. **Alignment of the cytoplasmic domains of EGFP fusion TLR4 truncation mutants used in this study.** TLR4 (766tr) signifies the mutant truncated at position 766. Others are named in the same manner. The amino acids are colored based on their physicochemical properties: *pink*, basic; *blue*, acidic; *green*, polar and neutral; and *orange*, hydrophobic. The *black overline* represents the TIR domain. *Colored overlines* indicate amino acid sequences identical to known sorting signal motifs except for two LLs, which are dileucine motif-like sequences in that they consist of solely two consecutive leucines without preceding aspartate or glutamate. *Capital letters* on the *line* signify the single-letter code for amino acids: *E*, glutamic acid; *L*, leucine; *R*, arginine; and *Y*, tyrosine. *X* signifies any amino acid, and Ø signifies an amino acid residue with a bulky hydrophobic side chain.

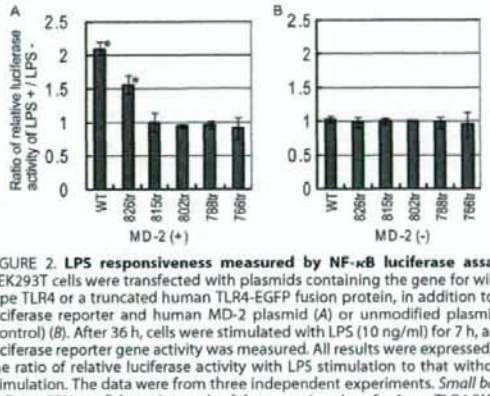

FIGURE 2. **LPS responsiveness measured by NF-κB luciferase assay.** HEK293T cells were transfected with plasmids containing the gene for wild-type TLR4 or a truncated human TLR4-EGFP fusion protein, in addition to a luciferase reporter and human MD-2 plasmid (*A*) or unmodified plasmids (control) (*B*). After 36 h, cells were stimulated with LPS (10 ng/ml) for 7 h, and luciferase reporter gene activity was measured. All results were expressed as the ratio of relative luciferase activity with LPS stimulation to that without stimulation. The data were from three independent experiments. *Small bars* indicate 95% confidence intervals of the mean (*p* values for * are: TLR4 (WT)-EGFP/MD-2 (+), $p = 0.002$; TLR4 (826tr)-EGFP/MD-2 (+), $p = 0.016$).

Statistical Analyses—All quantitative experiments were repeated three times, and each experiment was done in triplicate. The ratio of relative luciferase activity of LPS+ to LPS− was calculated as the index of the responsiveness to the stimuli as explained above. When positive response is observed, the ratio should significantly exceed one. The means of the ratio were represented in *bar graphs*. The 95% confidence interval of the mean of the ratio was calculated and indicated on each *bar* in the *graph*, and *p* values were calculated using Student's *t* distribution compared with the hypothetical mean, one.

RESULTS

Truncation Analysis of TLR 4—To identify amino acid sequences in the cytoplasmic tail of TLR4 that are involved in both signal transduction and subcellular distribution, first we generated five truncation mutants of TLR4 with a fluorescent protein (EGFP) at the C terminus of TLR4.

Although there are no known definite sorting signal motifs in the cytoplasmic tail of TLR4, some amino acid sequences are similar or identical to known general sorting signal motifs as shown in Fig. 1. *YXXØ*, a form of tyrosine-based sorting signal, and *EXXXLL*, a form of dileucine (LL)-based sorting signal, both control protein internalization, lysosomal targeting, and basolateral targeting (10), where "*X*" represents any amino acid, "Ø" stands for an amino acid residue with a bulky hydrophobic side chain, and other letters are single-letter abbreviations for the amino acids. "Diacidic" signals such as *DXE* mediate export from the ER (11). RR or *RXR* is another example of an ER export signal (12). Truncation sites were chosen so that some of these amino acid sequences were deleted in each mutant. Because the TIR domain, which is essential in TLR4 signaling and possibly subcellular localization (13), spans most of the cytoplasmic domain of TLR4, four out of five mutants have involvement in the TIR domain, which we hypothesized could result in impaired signal transduction and a change in subcellular distribution. Part of the cytoplasmic portion of the amino acid sequence of the truncation mutants is shown in Fig. 1. The five truncation mutant proteins lost their C-terminal tails at positions 826, 815, 802, 788, and 766, respectively, and were conjugated with EGFP *in vitro*. Actual truncation and ligation sites of all actual mutants were confirmed to have the designed DNA alignment by sequencing.

We utilized the luciferase reporter assay to assess NF-κB transcription activity as an indicator of TLR4 response to LPS stimuli. MD-2 is reported to be essential for this response (9). However, because it is not known whether MD-2 is necessary for transduction of the truncated TLR4 signal as well, we performed the assays with and without MD-2. The index of cell responsiveness to the stimulation was measured as the ratio between RLA with LPS stimulation and RLA without LPS stimulation. Only cells transfected with TLR4 (826tr)-EGFP in combination with MD-2 retained responsiveness to LPS stimulation. One exception was wild-type TLR4-EGFP (Fig. 2*A*). HEK293T cells transfected with TLR4 but without MD-2 did not respond to LPS stimuli regardless of the TLR4-EGFP genotype (Fig. 2*B*).

Next, we compared the localization of wild-type and truncated mutants of TLR4-EGFP in HEK293T by fluorescence microscopy (Fig. 3*A*). The wild-type TLR4 cotransfected with MD-2 was expressed on the plasma membrane and also in the

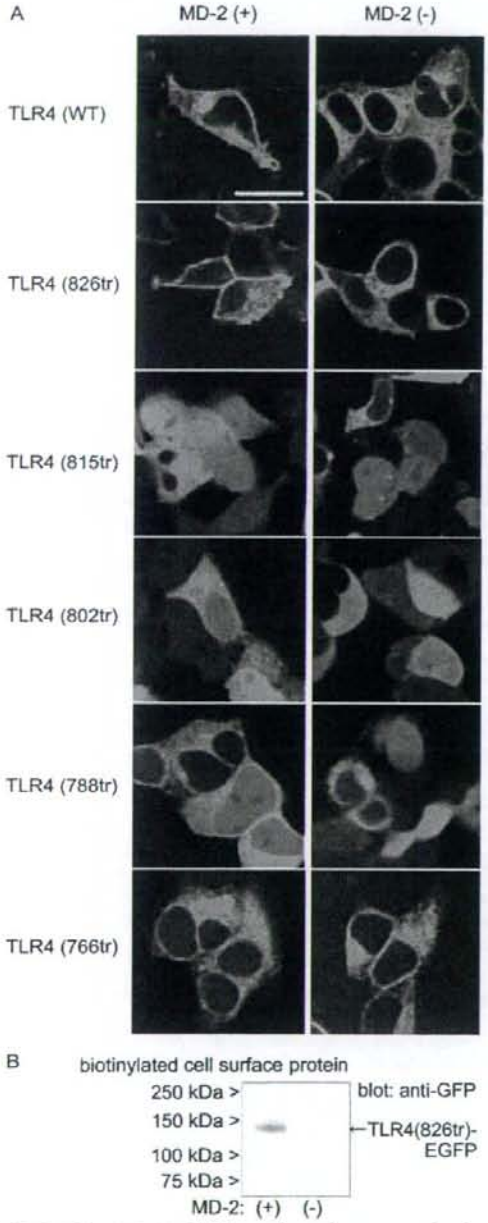

FIGURE 3. **Residues 815–826 of TLR4 contain a region necessary for plasma membrane localization.** *A*, cells were cultured on coverslips in 12-well plates and transfected as in Fig. 2. EGFP-tagged TLR4 was visualized by laser confocal microscopy. Fluorescence from EGFP was observed in *green*. Each genotype of TLR4-EGFP was cotransfected with a human MD-2 plasmid or empty vector. *Bar*, 20 μm. *B*, TLR4 (826tr)-EGFP with or without coexpression of MD-2 were tagged by biotinylation of the cell surface proteins and affinity-purified. TLR4 was visualized by immunoblotting using an anti-GFP monoclonal antibody. Samples from both combinations of DNAs were prepared from the same number of cells.

perinuclear area. These findings were consistent with observations by others (14, 15). TLR4 is reported to localize in the Golgi apparatus as well as on the plasma membrane. Our observation of TLR4-EGFP accumulation in the perinuclear area does not contradict the report that TLR4 partly localizes in the Golgi apparatus (14).

TLR4-EGFP truncation mutants, 815tr, 802tr, 788tr, and 766tr apparently did not localize at the plasma membrane. No particular fluorescence pattern that might be characteristic of localization to a specific intracellular compartment was observed. Only TLR4 (826tr)-EGFP, which has the shortest truncation, was expressed on the plasma membrane and in the perinuclear area, and the fluorescence pattern was similar to that of wild-type (Fig. 3*A*). No TLR4 genotypes, including wild-type TLR4-EGFP, clearly localized on the plasma membrane in the absence of MD-2 (Fig. 3*A*). MD-2 is reported to be necessary for localization of wild-type TLR4 at the plasma membrane (15), which is consistent with our observation. Intracellular distribution of mutant TLR4 varied depending on the genotype, but no particular cellular structure was identified as an alternative target site. Furthermore, we examined the plasma membrane expression of TLR4 (826tr)-EGFP by cell surface protein biotinylation. The expression level of TLR4 (826tr)-EGFP was markedly decreased without coexpression of MD-2 (Fig. 3*B*), which is compatible with the microscope observation.

Removal of the C-terminal segment of TLR4 at residue 826 does not qualitatively affect LPS responsiveness and subcellular distribution. However, when more residues, up to position 815, were removed, both signal transduction and plasma membrane localization were impaired. These results suggest that residues 815–826 of TLR4 contain at least one segment that is critical for those functions.

Amino Acid Sequence Replacement Analysis—To identify critical amino acid sequences in this region, we generated an amino acid replacement mutant of TLR4 instead of truncation mutants. As shown in Fig. 1, although it is not a canonical sequence, leucine-leucine at 815–816 partially fits a known sorting signal motif, a dileucine motif, (D/E)*XXX*L(L/I) or D*XX*LL, which plays an important role in internalization of plasma membrane protein or sorting from the *trans*-Golgi network (10). Thus, as has been done in a similar study (16), a mutant was generated in which alanines were substituted for both leucines at positions 815 and 816.

We measured the NF-κB activity of TLR4 (L815AL816A)-EGFP, the mutant in which both leucines were replaced with alanines, under LPS stimulation (Fig. 4*A*). This mutant protein did not respond to LPS stimuli. Microscopic observation revealed that TLR4 (L815AL816A)-EGFP was not expressed on the plasma membrane regardless of whether MD-2 was cotransfected (Fig. 4*B*). The phenotype of this doubly substituted mutant appeared to be the same as that of the truncation mutants. These results imply that the leucines in positions 815 and 816 play an important role in TLR4 plasma membrane localization.

Analysis of Single Amino Acid Substitution Mutants—As previously mentioned, the amino acid sequence leucine-leucine at positions 815 and 816 does not completely match the dileucine motif, *i.e.* it lacks a preceding acidic amino acid. Therefore it

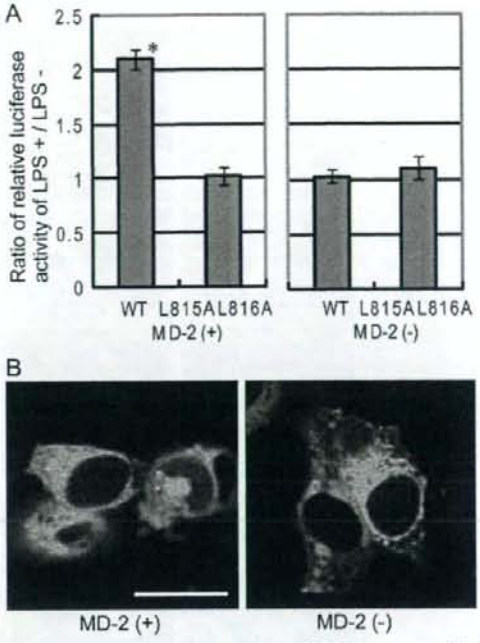

FIGURE 4. **Leucines at positions 815–816 of TLR4 are responsible for impairment of LPS responsiveness and plasma membrane expression.** *A*, the LPS stimulation assay was done for TLR4 (L815AL816A)-EGFP as in Fig. 2. The data were from three independent experiments. *Small bars* indicate 95% confidence intervals of the mean (p value for * are: TLR4 (WT)-EGFP/MD-2 (+), $p = 0.002$). *B*, TLR4 (L815AL816A)-EGFP expression in HEK293T cells was observed by laser confocal microscopy. *Bar*, 20 μm.

was reasonable to explore whether leucines 815 and 816 need to be adjacent to each other. We created five genotypes of single amino acid mutants of TLR4: TLR4 (K813A)-EGFP, TLR4 (L815A)-EGFP, TLR4 (L816A)-EGFP, and TLR4 (D817A)-EGFP. We excluded the amino acid at position 814 from the analysis, because the amino acid in position 814 of wild-type TLR4 is alanine. The amino acid sequence alignment of wild-type TLR4 and the single amino acid replacement mutants is shown in Fig. 5. DNA sequences were confirmed by sequencing.

As was done with truncation mutants, we measured NF-κB activity of wild-type TLR4-EGFP, TLR4 (K813A)-EGFP, TLR4 (L815A)-EGFP, TLR4 (L816A)-EGFP, and TLR4 (D817A)-EGFP in response to LPS stimulation. All mutants except TLR4 (L815A)-EGFP showed responsiveness to LPS stimulation with coexpression of MD-2 (Fig. 6*A*). Without MD-2, no genotype of TLR4-EGFP responded to LPS stimulation (Fig. 6*B*). LPS stimulation was performed in an identical manner as with truncation mutants.

We analyzed the subcellular distribution of single amino acid mutants of TLR4-EGFP with and without MD-2 coexpression by fluorescence microscopy. TLR4 (K813A)-EGFP and TLR4 (D817A)-EGFP showed a similar fluorescence pattern to the wild-type, which localized at the plasma membrane when coexpressed with MD-2. No genotypes of TLR4-EGFP localized on the plasma membrane without MD-2 (Fig. 7). The cells transfected with TLR4 (L815A)-EGFP coexpressed with MD-2 did not show plasma membrane fluorescent pattern. Also, TLR4 (L815A)-EGFP showed comparatively weaker fluoresce than other mutants, possibly due to lower expression of the protein. Fluorescence of TLR4 (L816A)-EGFP with MD-2 was ambiguous as for the plasma membrane expression. Some kind of membranous structure was observed in the cytoplasmic area, but the intensity of the plasma membrane green fluorescence was obscure. Together with the results from the LPS stimulation experiment, the leucines at positions 815 and 816 are considered to play important roles in signal transduction and/or subcellular distribution of TLR4.

Because EGFP consists of 239 amino acids, which is about one-third the size of the complete TLR4 protein, the experimental results obtained using TLR4-EGFP could have been influenced by the presence of the EGFP fused at the C terminus of TLR4. To rule out this possibility, we tested the functional integrity of both TLR4 (L815A) and TLR4 (L816A) with and without EGFP at the C terminus. Reporter assays were performed under the same conditions except that the shorter tag, FLAG-His_6, which has only 21-amino acid tags at the C terminus, was fused to TLR4 in place of EGFP. There was no difference

```
TLR4 (WT) EGFP    651VYKFYFHLMLLAGCIKYGRGENIYDAFVIYSSQDEDWVRNELVKNLEEGVPPFQLCLHYR
TLR4 (K813A) EGFP   VYKFYFHLMLLAGCIKYGRGENIYDAFVIYSSQDEDWVRNELVKNLEEGVPPFQLCLHYR
TLR4 (L815A) EGFP   VYKFYFHLMLLAGCIKYGRGENIYDAFVIYSSQDEDWVRNELVKNLEEGVPPFQLCLHYR
TLR4 (L816A) EGFP   VYKFYFHLMLLAGCIKYGRGENIYDAFVIYSSQDEDWVRNELVKNLEEGVPPFQLCLHYR
TLR4 (D817A) EGFP   VYKFYFHLMLLAGCIKYGRGENIYDAFVIYSSQDEDWVRNELVKNLEEGVPPFQLCLHYR
TLR4 (L815A-L816A) EGFP   VYKFYFHLMLLAGCIKYGRGENIYDAFVIYSSQDEDWVRNELVKNLEEGVPPFQLCLHYR

TLR4 (WT) EGFP    711DFIPGVAIAANIIHEGFHKSRKVIVVVSQHFIQSRWCIFEYEIAQTWQFLSSRAGIIFIV
TLR4 (K813A) EGFP   DFIPGVAIAANIIHEGFHKSRKVIVVVSQHFIQSRWCIFEYEIAQTWQFLSSRAGIIFIV
TLR4 (L815A) EGFP   DFIPGVAIAANIIHEGFHKSRKVIVVVSQHFIQSRWCIFEYEIAQTWQFLSSRAGIIFIV
TLR4 (L816A) EGFP   DFIPGVAIAANIIHEGFHKSRKVIVVVSQHFIQSRWCIFEYEIAQTWQFLSSRAGIIFIV
TLR4 (D817A) EGFP   DFIPGVAIAANIIHEGFHKSRKVIVVVSQHFIQSRWCIFEYEIAQTWQFLSSRAGIIFIV
TLR4 (L815A-L816A) EGFP   DFIPGVAIAANIIHEGFHKSRKVIVVVSQHFIQSRWCIFEYEIAQTWQFLSSRAGIIFIV

TLR4 (WT) EGFP    771LQKVEKTLLRQQVELYRLLSRNTYLEWEDSVLGRHIFWRRLRKALLDGKSWNPEGTVGTG
TLR4 (K813A) EGFP   LQKVEKTLLRQQVELYRLLSRNTYLEWEDSVLGRHIFWRRLRAALLDGKSWNPEGTVGTG
TLR4 (L815A) EGFP   LQKVEKTLLRQQVELYRLLSRNTYLEWEDSVLGRHIFWRRLRKAALDGKSWNPEGTVGTG
TLR4 (L816A) EGFP   LQKVEKTLLRQQVELYRLLSRNTYLEWEDSVLGRHIFWRRLRKALADGKSWNPEGTVGTG
TLR4 (D817A) EGFP   LQKVEKTLLRQQVELYRLLSRNTYLEWEDSVLGRHIFWRRLRKALLAGKSWNPEGTVGTG
TLR4 (L815A-L816A) EGFP   LQKVEKTLLRQQVELYRLLSRNTYLEWEDSVLGRHIFWRRLRKAAADGKSWNPEGTVGTG

TLR4 (WT) EGFP    831CNWQEATSIGSIATMVSKGEELFTGVVP.....
TLR4 (K813A) EGFP   CNWQEATSIGSIATMVSKGEELFTGVVP.....
TLR4 (L815A) EGFP   CNWQEATSIGSIATMVSKGEELFTGVVP.....
TLR4 (L816A) EGFP   CNWQEATSIGSIATMVSKGEELFTGVVP.....
TLR4 (D817A) EGFP   CNWQEATSIGSIATMVSKGEELFTGVVP.....
TLR4 (L815A-L816A) EGFP   CNWQEATSIGSIATMVSKGEELFTGVVP.....
                          TLR4 ---------- EGFP ---------->
```

FIGURE 5. **Alignment of the cytoplasmic domain of EGFP fusion TLR4 amino acid-replacement mutants used in this study.** TLR4 (L813A) signifies a mutant with leucine replaced with alanine at position 813. Others are named in the same manner. The amino acids are *colored* as in Fig. 1. All amino acids are designated using the single-letter code.

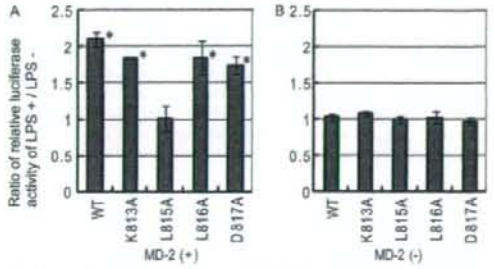

FIGURE 6. **Leucine at position 815 of TLR4 is pivotal for LPS responsiveness as measured by NF-κB luciferase assay.** *A*, HEK293T cells were transfected with single amino acid replacement mutants of the human TLR4-EGFP fusion protein plasmid, human MD-2 plasmid, and luciferase reporter and control plasmids. After 36 h, cells were stimulated with LPS (10 ng/ml) for 7 h, and luciferase reporter gene activity was measured. *B*, instead of MD-2, an empty vector was cotransfected with TLR4-EGFP plasmid and reporter assay vectors. LPS stimulation was done as in *A*. All results were expressed in the ratio of relative luciferase activity with LPS stimulation to that without the stimulation as in Fig. 2. The data were from three independent experiments. *Small bars* indicate 95% confidence intervals of the mean (*p* values for * are: TLR4 (WT)-EGFP/MD-2 (+), $p = 0.002$; TLR4 (K813A)-EGFP/MD-2 (+), $p = 0.000$; TLR4 (L816A)-EGFP/MD-2 (+), $p = 0.018$; and TLR4 (D817A)-EGFP/MD-2 (+), $p = 0.007$).

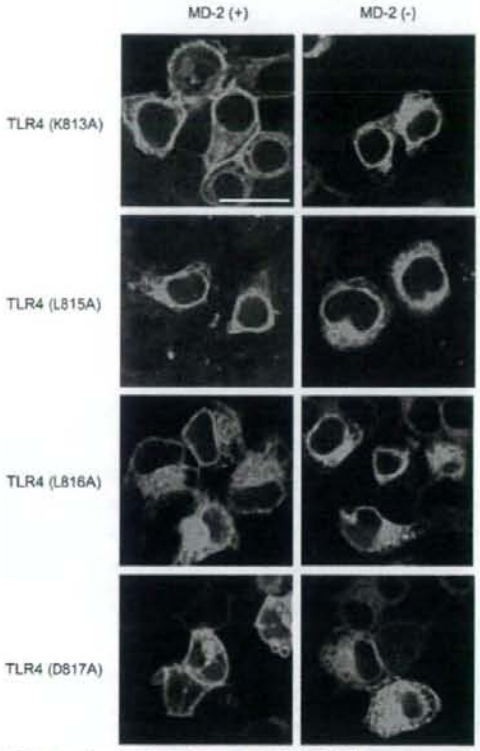

FIGURE 7. **Leucines at the position 815 and 816 of TLR4 are responsible for full plasma membrane expression.** Cells were cultured on coverslips in 12-well plates and transfected as in Fig. 2. EGFP-tagged TLR4 was visualized by laser confocal microscopy. Each genotype of TLR4-EGFP was cotransfected with human MD-2 plasmid or empty vector. *Bar*, 20 μm.

between EGFP-tagged proteins and FLAG-His_6-tagged proteins in the relative pattern of responsiveness against LPS stimulation (Fig. 8*A*). Because CD14 is also important for LPS recognition by TLR4, we examined the effect of CD14 coexpression on the phenotypic changes of the mutants (17, 18). Coexpression of CD14 did not change the phenotypes of wild-type TLR4, TLR4 (L815A), and TLR4 (L816A) in terms of LSP responsiveness (data not shown).

Cell surface expressions of the wild-type, L815A mutant, and L816A mutant TLR4-FLAG- His_6 fusion proteins were also examined. Live cells transfected with wild-type TLR4, the L815A mutant or the L816A mutant as well as human MD-2 and CD14 were biotinylated on the cell surface, and the biotinylated proteins were affinity-purified and subjected to Western blotting. Fig. 8*B* shows the marked difference in cell surface expression of wild-type and mutants L815A and L816A. Note that biotinylated proteins have additional residues on every amine of the extracellular domain, which leads to a band shift during electrophoresis. Although both mutants were detected far less than the wild-type on the cell surface, comparatively more L816A mutant was expressed on the plasma membrane than L815A mutant, and the amount of L815A mutant seemed to be negligible compared with the wild type. These results may clarify the ambiguity of the microscopic observation of TLR4 (L815A) and TLR4 (L816A). Plasma membrane expression of TLR4 was impaired when the leucine at 815 or 816 was replaced to alanine. But the leucine at 815 is more critical, and the mutant L816A may show the weaker phenotypic change.

To further investigate the characteristics of the TLR4 (L815A) mutant, we performed an immunoprecipitation assay of wild-type and mutant TLR4. Cells were transfected with a human MD-2-FLAG-His_6 expression vector and either the wild-type or the mutant (L815A) TLR4-EGFP expression vector. Anti-TLR4 monoclonal antibody (clone HTA125), anti-GFP polyclonal antibody, or anti-FLAG monoclonal antibody was added to the lysate and precipitated with Protein G-Sepharose beads. Collected proteins were eluted and subjected to Western blotting. The results are shown in Fig. 8*C*. TLR4 (L815A) was not immunoprecipitated with anti-TLR4 antibody (HTA125). HTA125 antibody was raised against TLR4-expressing cells (9) and recognizes the extracellular portion of TLR4. This result suggests that the amino acid replacement at position 815 may cause a change in the extracellular portion of TLR4 and/or that the replacement may also inhibit cell surface expression of the mutant protein. On the other hand, both wild-type TLR4-EGFP and mutant TLR4-EGFP were immunoprecipitated with anti-GFP polyclonal antibody, which recognized EGFP. However, of the two bands of TLR4, the heavier band seems to be somewhat faint in the mutant, whereas in the wild type the heavier band is at least as dense as the lighter one. TLR4 can be detected as two separate bands in a Western blot (19), especially under transient transfection conditions. The difference in proportion of the heavy and light bands between wild-type and mutant TLR4 may suggest that there is some difference in glycosylation. Furthermore, wild-type TLR4 was coprecipitated with MD-2-FLAG-His_6, but the mutant TLR4 could not be detected (Fig. 8*C*, *lanes 4* and *8*). Because MD-2 is

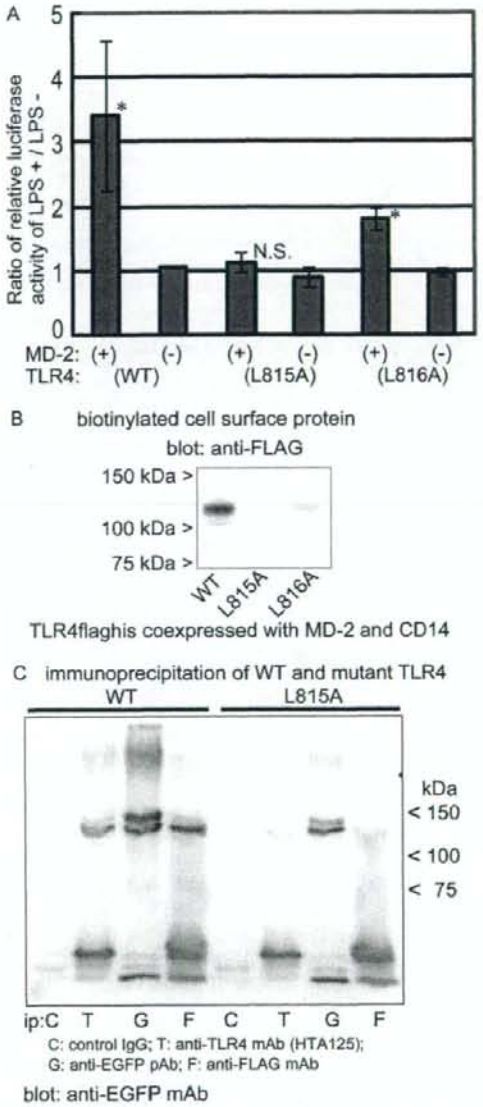

FIGURE 8. *A*, TLR4 mutants L815A and L816A with and without EGFP fusion exhibit the same phenotypes in LPS responsiveness and plasma membrane expression. HEK293T cells were transfected with the wild-type, the L815A or L816A mutant TLR4flaghis plasmid plus the human MD-2 plasmid and luciferase reporter, or control plasmids. After 36 h, cells were stimulated with LPS (10 ng/ml) for 7 h, and luciferase reporter gene activity was measured. The data were from three independent experiments. *Small bars* indicate 95% confidence intervals of the mean (p values for * are: TLR4 (WT) flaghis/MD-2 (+), $p = 0.046$; TLR4 (L816A) flaghis/MD-2 (+), $p = 0.003$). *N.S.*: not significant. *B*, wild-type and mutant TLR4s L815A and L816A were tagged by biotinylation of the cell surface proteins and affinity-purified. Human MD-2 and CD14 were coexpressed. TLR4 was visualized by immunoblotting using an anti-FLAG monoclonal antibody (*mAb*). Faint bands below 100 kDa are considered to be unbiotinylated intracellular TLR4 proteins that were not washed off during the process. Samples from TLR4 (WT), TLR4 (L815A), and TLR4 (L816A), respectively, were prepared from the same number of cells as for the biotinylation experiment. *C*, immunoprecipitation with antibodies further reveals the characteristics of TLR4 (L815A). Anti-TLR4 monoclonal antibody (HTA125) does not precipitate the mutant TLR4, whereas anti-GFP polyclonal antibody (*pAb*) precipitates both wild-type and mutant TLR4. Mutant TLR4 was not coprecipitated with MD-2-FLAG-His_6. Lysates were prepared from cells transiently expressing wild-type or mutant TLR4-EGFP and MD-2-FLAG-His_6.

associated with TLR4 (9), it is logical to expect that immunoprecipitating MD-2-FLAG-His_6 with anti-FLAG antibody should cause TLR4 to be coprecipitated with it. It is suggested by the result here that the association of the TLR4 mutant with MD-2 is impaired.

DISCUSSION

In this research, we performed mutagenesis analyses of particular amino acid residues in TLR4 to explore the mechanisms of TLR4 intracellular signal transduction and subcellular distribution. We found the candidate residues by analyzing truncation mutants of TLR4 in the cytoplasmic region, in which both signaling and normal subcellular distribution of TLR4 are disturbed. Because we are focusing on a common mechanism for the impaired signaling and distribution, we finally picked a single amino acid mutant that does not respond to LPS stimuli, as measured with NF-κB reporter luciferase assay, and one that does not localize on the plasma membrane. TLR4 (L815A) is a mutant that meets these conditions, and our results suggest that the leucine at position 815 of TLR4 is required for both signal transduction and plasma membrane localization.

The best known single amino acid mutant of TLR4 is TLR4 (P712H) known as the *Lps*^{d} mutation in the C3H/HeJ mouse, which corresponds to position 714 in this study of human TLR4 (5, 6, 20). Mice carrying this mutation opened up the rediscovery of TLR4 as a key player in innate immunity. Because this proline residue at this position is within the TIR domain and is conserved among TLRs or TLR4s of other species, it is assumed that the residue plays an important role in TLR4 function. The association of TLR4 (P712H) with its adapter proteins is reported to be intact, and the explanation for the functional impairment of TLR4 (P712H) is not clear (21–23).

Some single amino acid variants are found in humans, and these are related to the incidence or prognosis of some infections and other diseases. A growing body of data suggests that the ability of certain individuals to respond properly to TLR4 ligands may be impaired by single-nucleotide polymorphisms within TLR4 genes (24). The D299G and T399I alleles of the TLR4 gene have been associated with increased risk of severe infections (25).

By clarifying the subcellular component where the mutant protein is retained, or by clarifying to which compartment the mutant is not delivered, the abnormal intracellular sorting that is caused by the mutation in TLR4 (L815A) could be elucidated more precisely. Usually a sorting signal motif is comprised of several amino acids. In this regard, if the leucine at position 815 is a part of a motif, there should be other amino acids that are also members of the motif. Although replacement of leucine with alanine at position 816 did not cause an apparent signal transduction impediment, plasma membrane expression of TLR4 (L816A) was impaired to a certain extent. Positive

response to LPS stimulation by TLR4(L816A) could be attributable to this small amount of expression on the plasma membrane. Mutagenesis analyses of neighboring amino acids of the leucine at 815 were not definitive, but the results could be suggestive that the adjacent leucine at 816 may work together with the leucine at 815. Leucines at position 815 and 816 could be in the same motif, and the leucine at position 816 may be less critical.

Several proteins have been reported to be involved in TLR4 cell surface expression. Heat shock protein gp96 is necessary for TLR4 association with MD-2 in the ER and for subsequent cell surface expression (26). PRAT4A and PRAT4B are associated with TLR4 and regulate TLR4 cell surface expression (27, 28). In embryonic fibroblasts of MD-2 knockout mice, TLR4 localization on the cell surface is severely impaired, and most TLR4 is retained in the ER or Golgi apparatus (15). MD-2 binds to TLR4 at its extracellular domain and is essential for LPS recognition by TLR4 (29). Although proteins such as CD14 and LPS-binding protein are reported to have important roles in LPS recognition by TLR4, in an *in vitro* setting HEK293T cells gain LPS responsiveness by introducing only TLR4 and MD-2 genes when measured by NF-κB reporter assay (9, 30). Without transfection, HEK293 cells do not express TLR4, MD-2, or CD14, which are involved in LPS-induced intracellular signaling (31, 32). In this study, we show that the association of the TLR4 mutant and MD-2 is impaired (Fig. 8*C*).

Post-translational modification is another important factor for TLR4 function. Asparagine residues in the extracellular portion of TLR4 need to be glycosylated for plasma membrane expression of TLR4 (15, 19, 33). TLR4·MD-2 association is necessary for this glycosylation as well. The difference in the proportion of the heavy band to lighter band between wild-type and L815A mutant TLR4 immunoprecipitated with anti-GFP polyclonal antibody suggests that there may be some difference in glycosylation between wild-type and L815A mutant TLR4 (Fig. 8*C*). Although leucine at position 815 is located in the cytoplasmic tail of TLR4, we speculated that substitution of leucine at position 815 may cause a conformational change in the extracellular portion of the protein, which may interfere with the association between L815A mutant TLR4 and MD-2, leading to inhibition of glycosylation and cell surface expression of the mutant protein. Further investigation may reveal the mechanism involved in this phenotypic change in TLR4 (L815A), which would lead to better understanding of the mechanism of wild-type TLR4 signaling and trafficking.

Acknowledgment—We greatly appreciate the gift of human TLR4 and MD-2 cDNA from Dr. Kensuke Miyake (Institute of Medical Science, University of Tokyo, Japan).

REFERENCES

1. Takeda, K., Kaisho, T., and Akira, S. (2003) *Annu. Rev. Immunol.* **21,** 335–376
2. Hoebe, K., Du, X., Georgel, P., Janssen, E., Tabeta, K., Kim, S. O., Goode, J., Lin, P., Mann, N., Mudd, S., Crozat, K., Sovath, S., Han, J., and Beutler, B. (2003) *Nature* **424,** 743–748
3. Oshiumi, H., Sasai, M., Shida, K., Fujita, T., Matsumoto, M., and Seya, T. (2003) *J. Biol. Chem.* **278,** 49751–49762
4. Yamamoto, M., Sato, S., Mori, K., Hoshino, K., Takeuchi, O., Takeda, K., and Akira, S. (2002) *J. Immunol.* **169,** 6668–6672
5. Qureshi, S. T., Lariviere, L., Leveque, G., Clermont, S., Moore, K. J., Gros, P., and Malo, D. (1999) *J. Exp. Med.* **189,** 615–625
6. Poltorak, A., He, X., Smirnova, I., Liu, M. Y., Van Huffel, C., Du, X., Birdwell, D., Alejos, E., Silva, M., Galanos, C., Freudenberg, M., Ricciardi-Castagnoli, P., Layton, B., and Beutler, B. (1998) *Science* **282,** 2085–2088
7. Visintin, A., Mazzoni, A., Spitzer, J. A., and Segal, D. M. (2001) *Proc. Natl. Acad. Sci. U. S. A.* **98,** 12156–12161
8. Nishitani, C., Mitsuzawa, H., Hyakushima, N., Sano, H., Matsushima, N., and Kuroki, Y. (2005) *Biochem. Biophys. Res. Commun.* **328,** 586–590
9. Shimazu, R., Akashi, S., Ogata, H., Nagai, Y., Fukudome, K., Miyake, K., and Kimoto, M. (1999) *J. Exp. Med.* **189,** 1777–1782
10. Bonifacino, J. S., and Traub, L. M. (2003) *Annu. Rev. Biochem.* **72,** 395–447
11. Nishimura, N., and Balch, W. E. (1997) *Science* **277,** 556–558
12. Nufer, O., and Hauri, H. P. (2003) *Curr. Biol.* **13,** R391–393
13. Slack, J. L., Schooley, K., Bonnert, T. P., Mitcham, J. L., Qwarnstrom, E. E., Sims, J. E., and Dower, S. K. (2000) *J. Biol. Chem.* **275,** 4670–4678
14. Latz, E., Visintin, A., Lien, E., Fitzgerald, K. A., Monks, B. G., Kurt-Jones, E. A., Golenbock, D. T., and Espevik, T. (2002) *J. Biol. Chem.* **277,** 47834–47843
15. Nagai, Y., Akashi, S., Nagafuku, M., Ogata, M., Iwakura, Y., Akira, S., Kitamura, T., Kosugi, A., Kimoto, M., and Miyake, K. (2002) *Nat. Immunol.* **3,** 667–672
16. Hein, C., and Andre, B. (1997) *Mol. Microbiol.* **24,** 607–616
17. Beutler, B. (2000) *Curr. Opin. Immunol.* **12,** 20–26
18. Akashi, S., Ogata, H., Kirikae, F., Kirikae, T., Kawasaki, K., Nishijima, M., Shimazu, R., Nagai, Y., Fukudome, K., Kimoto, M., and Miyake, K. (2000) *Biochem. Biophys. Res. Commun.* **268,** 172–177
19. Ohnishi, T., Muroi, M., and Tanamoto, K. (2003) *Clin. Diagn. Lab. Immunol.* **10,** 405–410
20. Xu, Y., Tao, X., Shen, B., Horng, T., Medzhitov, R., Manley, J. L., and Tong, L. (2000) *Nature* **408,** 111–115
21. Dunne, A., Ejdeback, M., Ludidi, P. L., O'Neill, L. A., and Gay, N. J. (2003) *J. Biol. Chem.* **278,** 41443–41451
22. Fitzgerald, K. A., Palsson-McDermott, E. M., Bowie, A. G., Jefferies, C. A., Mansell, A. S., Brady, G., Brint, E., Dunne, A., Gray, P., Harte, M. T., McMurray, D., Smith, D. E., Sims, J. E., Bird, T. A., and O'Neill, L. A. (2001) *Nature* **413,** 78–83
23. Horng, T., Barton, G. M., and Medzhitov, R. (2001) *Nat. Immunol.* **2,** 835–841
24. Schroder, N. W., and Schumann, R. R. (2005) *Lancet Infect. Dis.* **5,** 156–164
25. Agnese, D. M., Calvano, J. E., Hahm, S. J., Coyle, S. M., Corbett, S. A., Calvano, S. E., and Lowry, S. F. (2002) *J. Infect. Dis.* **186,** 1522–1525
26. Randow, F., and Seed, B. (2001) *Nat. Cell Biol.* **3,** 891–896
27. Wakabayashi, Y., Kobayashi, M., Akashi-Takamura, S., Tanimura, N., Konno, K., Takahashi, K., Ishii, T., Mizutani, T., Iba, H., Kouro, T., Takaki, S., Takatsu, K., Oda, Y., Ishihama, Y., Saitoh, S., and Miyake, K. (2006) *J. Immunol.* **177,** 1772–1779
28. Konno, K., Wakabayashi, Y., Akashi-Takamura, S., Ishii, T., Kobayashi, M., Takahashi, K., Kusumoto, Y., Saitoh, S., Yoshizawa, Y., and Miyake, K. (2006) *Biochem. Biophys. Res. Commun.* **339,** 1076–1082
29. Nishitani, C., Mitsuzawa, H., Sano, H., Shimizu, T., Matsushima, N., and Kuroki, Y. (2006) *J. Biol. Chem.* **281,** 38322–38329
30. Akashi, S., Shimazu, R., Ogata, H., Nagai, Y., Takeda, K., Kimoto, M., and Miyake, K. (2000) *J. Immunol.* **164,** 3471–3475
31. Espevik, T., Latz, E., Lien, E., Monks, B., and Golenbock, D. T. (2003) *Scand. J. Infect. Dis.* **35,** 660–664
32. Muta, T., and Takeshige, K. (2001) *Eur. J. Biochem.* **268,** 4580–4589
33. da Silva Correia, J., and Ulevitch, R. J. (2002) *J. Biol. Chem.* **277,** 1845–1854

ARTICLE IN PRESS

EJP-65642; No of Pages 6

European Journal of Pharmacology xxx (2009) xxx–xxx

Contents lists available at ScienceDirect

European Journal of Pharmacology

journal homepage: www.elsevier.com/locate/ejphar

Cardiovascular Pharmacology

Administration of angiotensin II, but not catecholamines, induces accumulation of lipids in the rat heart

Makiko Hongo [a], Nobukazu Ishizaka [a,*], Kyoko Furuta [a], Naoya Yahagi [b], Kan Saito [a], Ryota Sakurai [a], Gen Matsuzaki [a], Kazuhiko Koike [c], Ryozo Nagai [a]

[a] Department of Cardiovascular Medicine, University of Tokyo, Graduate School of Medicine, Hongo 7-3-1, Bunkyo-ku, Tokyo 113-8655, Japan
[b] Department of Diabetes and Metabolic Disease, University of Tokyo, Graduate School of Medicine, Hongo 7-3-1, Bunkyo-ku, Tokyo 113-8655, Japan
[c] Department of Infectious Disease, University of Tokyo, Graduate School of Medicine, Hongo 7-3-1, Bunkyo-ku, Tokyo 113-8655, Japan

ARTICLE INFO

Article history:
Received 9 May 2008
Received in revised form 20 November 2008
Accepted 3 December 2008
Available online xxxx

Keywords:
Angiotensin II
Lipid accumulation
Lipotoxicity
Gene expression

ABSTRACT

Accumulation of lipids in the heart may cause cardiac dysfunction in various disorders, such as obesity and diabetes. In the current study, we have investigated whether administration of angiotensin II or norepinephrine induces accumulation of lipids and/or changes in the expression of genes related to lipid metabolism in the rat heart. Lipid deposition was found in myocardial, vascular wall, and perivascular cells of the angiotensin II-infused rat heart, and superoxide generation was increased in these lipid-positive cells. By contrast, intracardiac lipid deposition was not found in the heart of norepinephrine-induced hypertensive rats. Triglyceride content in the heart tissue of angiotensin II-infused rats increased more than 3-fold as compared with untreated controls. Losartan completely, but hydralazine only partially, suppressed the angiotensin II-induced intracardiac lipid deposition and increase in tissue triglyceride content. Administration of angiotensin II upregulated the mRNA expression of sterol regulatory element-binding protein-1c and fatty acid synthase, but downregulated that of uncoupling protein 2 and 3, in a manner dependent on the angiotensin AT_1 receptor. Collectively, these results suggest that angiotensin II may be involved in modulating both intracardiac lipid content and lipid metabolism-related gene expression, in part via an angiotensin AT_1 receptor-dependent and pressor-independent mechanism.

1. Introduction

Accumulation of lipids in non-adipose tissues can occur in certain disease conditions, including aging, over-nutrition, obesity, and diabetes, and may play a crucial role in the pathogenesis of tissue damage (Schaffer, 2003), a phenomenon referred to as lipotoxicity (Unger, 2002). Inappropriate accumulation of free fatty acids and neutral lipids can also be observed in the myocardium; this accumulation may result in both functional and morphological damage, such as systolic and/or diastolic dysfunction of the left ventricle (Chiu et al., 2005, Zhou et al., 2000), ventricular wall hypertrophy (Finck et al., 2003, Horiuchi et al., 1993), and interstitial fibrosis (Lee et al., 2004). In previous studies, we found that administration of angiotensin II to rats causes deposition of lipids in tubular epithelial and vascular wall cells in the kidney (Ishizaka et al., 2006, Saito et al., 2005), where cellular proliferation may be promoted. In the current study, we have investigated whether administration of two different pressor agents, angiotensin II and a catecholamine, causes intracardiac accumulation of lipids, and modulates the expression of genes related to lipid metabolism.

2. Materials and methods

2.1. Animal models

The experiments were performed in accordance with the guidelines for animal experimentation approved by the Animal Center for Biomedical Research, Faculty of Medicine, University of Tokyo. Angiotensin II-induced hypertension was induced in male Sprague-Dawley rats (250 to 300 g) by subcutaneous implantation of an osmotic minipump (Alza Pharmaceutical) as described previously (Ishizaka et al., 1997). Briefly, Val^5-angiotensin II (Sigma Chemical) was infused at doses of 0.7 mg/kg/day. Norepinephrine (Sigma Chemical) was infused at a dose of 2.8 mg/kg/day for 7 days using the same system. In some angiotensin II-infused rats, angiotensin AT_1 receptor antagonist, losartan (25 mg/kg/day), or the nonspecific vasodilator, hydralazine (15 mg/kg/day) (Sigma Chemical), both of which normalized the blood pressure of angiotensin II-infused rats, was given in the drinking water (Ishizaka et al., 2002).

* Corresponding author. Department of Cardiovascular Medicine, University of Tokyo, Graduate School of Medicine, Hongo 7-3-1, Bunkyo-ku, Tokyo 113-8655, Japan. Tel.: +81 3 3815 5411x3016; fax: +81 3 3974 2236.
E-mail address: nobuishizka-tky@umin.ac.jp (N. Ishizaka).

0014-2999/$ – see front matter © 2009 Elsevier B.V. All rights reserved.
doi:10.1016/j.ejphar.2008.12.006

Please cite this article as: Hongo, M., et al., Administration of angiotensin II, but not catecholamines, induces accumulation of lipids in the rat heart, Eur. J. Pharmacol. (2009), doi:10.1016/j.ejphar.2008.12.006

Table 1
Oligonucleotide primers used in this study

Gene	GenBank no.	Forward primer	Reverse primer
PPAR-α	NM_013196	GTGGCTGCTATAATTTGCTG	TGAAGGAGTTTTGGGAAGAG
PPAR-γ	NM_013124	ATCAGCTCTGTGGACCTCTC	AGGCTCTACTTTGATCGCAC
SREBP-1c	XM_213329	CTGATGGAGACAGGGAGTTC	ATCACCACGGCTGTCAGT
FAS	M76767	CTGGAACGTGAACATGATCT	TTCACCAGCAGGATACTCAG
HMG-CoA reductase	NM_013134	GACACTTACAATCTGTATGATG	CTTGGAGAGGTAAAACTGCCA
CPT-1	NM_031559	ATCGACCGCCATCTCTTC	CTCAAAGTCAAAGAGCTCCAC
CPT-2	NM_012930	TGACCAAAGAAGCAGCGAT	TTGTGGTTCATCTGCTGGTA
DGAT-1	NM_053437	TCTTCCTACCGGGATGTCAATC	TCCCTGCAGACACAGCTTTG
PGC-1α	AY237127	TCATTACCTACCGTTACACCT	CATACTTGCTCTTGGTGGAA
UCP2	BC062230	TGGTCGGAGATACCAGAG	GTCTGTCATGAGGTTGGCT
UCP3	AF035973	GTCCGATTTCAAGCCATGAT	CTTGTGATGTTGGGCCAAGT
Nox1	MN_053683	TGGACGAATTAGGCAAACCG	TTGGGGTGGGCAGTAGCTAT
Nox4	AY027527	AACACTGGTGAAGATTTGC	CTGAGGGATGATTGATTACTG
GAPDH	NM_017008	TGAACGGGAAGCTCACTGG	TCCACCACCCTGTTGCTGTA

PPAR, peroxisome proliferator-activated receptor; SREBP, sterol regulatory element-binding protein; FAS, fatty acid synthase; HMG-CoAR, 3-hydroxy-3-methylglutaryl coenzyme A reductase; CPT, carnitine palmitoyltransferase; DGAT, diacylglycerol acyltransferase; PGC, PPAR-γ coactivator; UCP, uncoupling protein; and GAPDH, glyceraldehyde-3-phosphate dehydrogenase.

2.2. Measurement of lipid contents in the serum and the heart

Serum levels of total cholesterol, triglycerides, and nonesterified fatty acid were measured by enzymatic methods (SRL). Contents of triglycerides, total cholesterol, and free cholesterol in the heart tissue were measured from homogenate extracts by enzymatic colorimetric determination using Triglyceride-E Test, Cholesterol-E Test, and Free cholesterol-E Test Wako, respectively (Wako Pure Chemicals).

2.3. Histological analysis

Oil red O staining was performed on sections of unfixed, freshly frozen heart samples (3 μm in thickness). The areas of lipid deposition were calculated by using the image analysis software, Photoshop (Adobe), and semiquantification of the lipid deposition was performed as described elsewhere (Ishizaka et al., 2006). Staining with the oxidative fluorescent dye dihydroethidium (DHE) was performed as described previously (Saito et al., 2004). Images were obtained with a fluorescent microscope BX51 (Olympus), and the fluorescence intensity, obtained from at least five fields for each section, was presented as the percentage of that of untreated control.

2.4. Western blot analysis

Western blot analysis was performed as described previously (Aizawa et al., 2000). Antibodies against total and phosphorylated forms AMP-activated protein kinase (Cell Signaling), sterol regulatory element-binding protein (SREBP)-1 (Santa Cruz Biotechnology), SREBP-2 (Santa Cruz Biotechnology), ATP-binding cassette transporter subfamily A1 (ABCA1) (Novus Biologicals), scavenger receptor class B type 1 (SR-B1) (Novus Biologicals), and mitochondrial superoxide dismutase (mt SOD) (Upstate) were used at a dilution of 1/1000.

2.5. Real time reverse transcription-polymerase chain reaction (RT-PCR)

Expression of lipid metabolism-related gene mRNA was analyzed by real time quantitative PCR performed by LightCycler together with hybriprobe technology (Roche Diagnostics). Expression of target genes was normalized to the mRNA expression of endogenous control, glyceraldehyde-3-phosphate dehydrogenase (GAPDH). The target genes were as follows: peroxisome proliferator-activated receptor (PPAR)-α (Nihon Gene Research Lab's Inc., Sendai, Japan), PPAR-γ, SREBP-1c, fatty acid synthase (FAS), 3-hydroxy-3-methylglutaryl coenzyme A reductase (HMG-CoAR), carnitine palmitoyltransferase (CPT)-1, CPT-2, diacylglycerol acyltransferase (DGAT)-1, PPAR-γ coactivator (PGC)-1α, uncoupling protein (UCP)2, UCP3, Nox1, and Nox4. The forward and backward primers used are described in Table 1.

2.6. Statistical analysis

Data are expressed as the mean±S. E. M. We used ANOVA followed by a multiple comparison test to compare raw data, before expressing the results as a percentage of the control value using the statistical analysis software StatView ver. 5.0 (SAS Institute). A value of $P<0.05$ was considered to be statistically significant.

3. Results

3.1. Characteristics of experimental animals

The hemodynamic parameters in each group have been reported elsewhere (Aizawa et al., 2000). Angiotensin II and norepinephrine elevated the blood pressure to a similar extent, and both hydralazine and losartan completely suppressed the blood pressure elevation induced by angiotensin II. Angiotensin II, but not norepinephrine, significantly increased the serum levels of triglycerides and non-esterified fatty acids, and these increases were inhibited by losartan, but not by hydralazine (Fig. 1A–C).

3.2. Tissue contents of lipids

The tissue content of triglycerides, total cholesterol, and free cholesterol was found to be increased in the heart of angiotensin II-

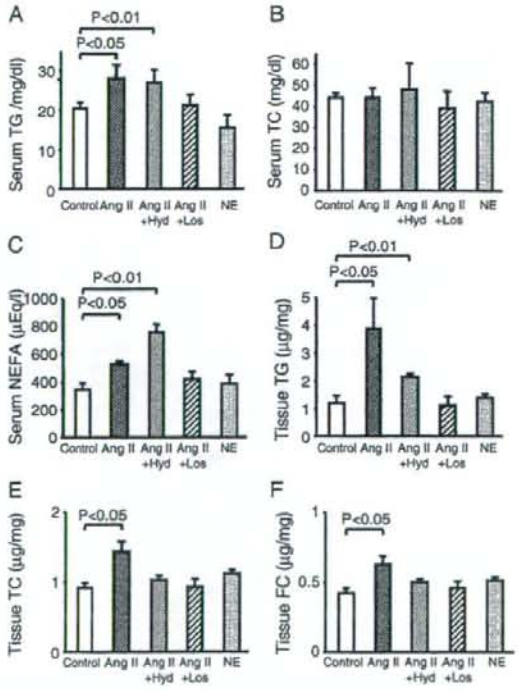

Fig. 1. Serum levels and tissue content of lipids. A–C. Serum levels of triglycerides (TG) (A), total cholesterol (TC) (B), and non-esterified fatty acids (NEFA) (C). D–E. Content of triglycerides (D), total cholesterol (E), free cholesterol (FC) (F) in the heart tissue. Shown in a summary of data from 4–6 rats in each group. Ang II, angiotensin II; Hyd, hydralazine; Los, losartan; and NE, norepinephrine.

Please cite this article as: Hongo, M., et al., Administration of angiotensin II, but not catecholamines, induces accumulation of lipids in the rat heart, Eur. J. Pharmacol. (2009), doi:10.1016/j.ejphar.2008.12.006

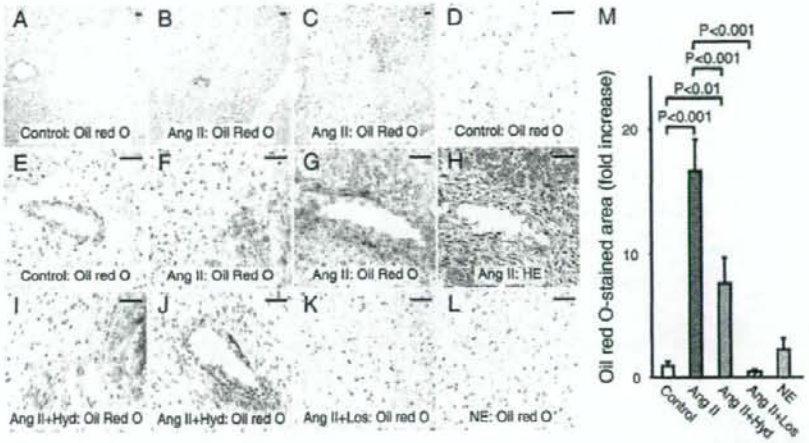

Fig. 2. Accumulation of lipids in the heart. A, D, E. Heart section from a control rat. B, C, F–H. Heart sections from angiotensin II (Ang II)-infused rats. I, J. Heart section from a rat given both angiotensin II and hydralazine (Hyd). K. Heart section from a rat given both angiotensin II and losartan (Los). L. Heart section from a rat given norepinephrine (NE). F and G are serial sections. A–G, I–L. Oil red O staining. H. Hematoxylin eosin (HE) staining. Lipid droplets were not observed in the myocardium or vascular regions (A, D, E) of control rats. Lipid droplets were present in both the myocardium (B, C, F) and perivascular regions (G) in the heart of angiotensin II-infused rats. Lipid droplets in the myocardium (I) and perivascular regions (J) were observed in the heart of rats given both angiotensin II and hydralazine, but not in the heart of rats given angiotensin II plus losartan (K) or those given norepinephrine (L). Original magnification, ×100 (A–C), and ×200 (D–L). Scale bars indicate 50 μm. M. Semiquantification of the oil red O-stained area. Shown is a summary of data from 5–7 experiments in each group.

infused rats, but not norepinephrine-infused rats (Fig. 1). Hydralazine only partially suppressed the angiotensin II-induced increase in intracardiac triglyceride content, but it completely suppressed the increase in intracardiac total cholesterol and free cholesterol content (Fig. 1D–F). Losartan suppressed the angiotensin II-induced increase in all three lipid fractions tested. Administration of losartan alone or hydralazine alone did not significantly alter the lipid content of the heart (losartan: triglycerides, 1.53±0.12 μg/mg, $n=4$; total cholesterol, 1.16±0.07 μg/mg, $n=3$; free cholesterol, 0.53±0.04 μg/mg, $n=4$; hydralazine: triglycerides, 1.40±0.14 μg/mg, $n=4$; total cholesterol, 1.09±0.14 μg/mg, $n=4$; free cholesterol, 0.43±0.04 μg/mg, $n=5$).

3.3. Staining for lipids

Oil red O staining of heart sections showed no apparent lipid deposition in the heart of untreated rats (Fig. 2A, D, E). By contrast, accumulation of oil red O-stainable lipid was observed in the myocardium as well as the arterial wall of angiotensin II-infused rats (Fig. 2B, C, F, G). In the angiotensin II-infused rat heart, lipid accumulation was also observed in perivascular regions, especially where remodeling of perivascular regions was apparent (Fig. 2G, H), and in granulation regions (data not shown). Lipid deposition remained present in the heart when angiotensin II-infused rats were concomitantly treated with hydralazine (Fig. 2I, J). On the other hand, lipid deposition was not apparent, or was very minor when present, in heart sections from rats treated with both angiotensin II and losartan or from rats treated with norepinephrine infusion (Fig. 2K, L). Semiquantitative measurements of the oil red O-stained areas are summarized in Fig. 2M.

3.4. Co-localization of lipid deposition and superoxide

As compared with untreated controls, DHE staining-positive signals were increased in the heart of angiotensin II-infused rats, and

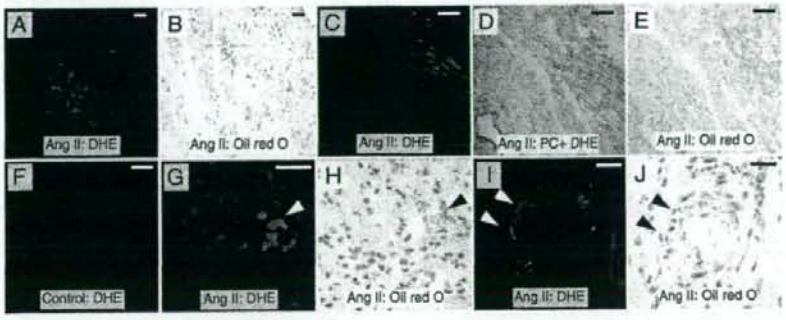

Fig. 3. Lipid and superoxide staining of the heart section. A–E, F–J. Heart sections from angiotensin (Ang) II-infused rats. F. Heart section from a control rat. A, C, F, G, I Dihydroethidium (DHE) staining. D. Phase contrast (PC) microscopic image overlaid with DHE staining image. B, E, H, J. Oil red O staining. C and D are the same section. C (=D)–E, G–H, and I–J are serial sections. Some cells with intense DHE staining (arrowheads in G and I) contained lipid deposits (arrowheads in H and J). Original magnification, ×100 (A–C), ×200 (C–H), and ×400 (I, J). Scale bars indicate 50 μm.

Please cite this article as: Hongo, M., et al., Administration of angiotensin II, but not catecholamines, induces accumulation of lipids in the rat heart, Eur. J. Pharmacol. (2009), doi:10.1016/j.ejphar.2008.12.006

Table 2
mRNA levels of genes related to lipid metabolism

Gene	Control (n=6)	Ang II (n=6)	P	Ang II+Hyd (n=5)	P	Ang II+Los (n=6)	P	NE (n=7)	P
PPAR-α	1±0.17	1.88±0.34	0.030	2.99±0.64	0.005	1.41±0.20	0.080	2.00±0.18	0.001
PPAR-γ	1±0.17	3.30±0.98	0.019	4.25±1.13	0.032	0.83±0.09	0.19	3.56±0.44	<0.001
SREBP-1c	1±0.24	3.66±1.02	0.008	2.67±0.96	0.039	0.71±0.12	0.14	0.77±0.17	0.21
FAS	1±0.17	2.97±0.32	<0.001	3.46±1.00	<0.001	1.30±0.17	0.18	1.28±0.13	0.18
HMG-CoA reductase	1±0.20	2.29±0.30	<0.001	2.50±0.66	0.009	0.99±0.23	0.49	0.98±0.33	0.48
CPT-1	1±0.06	0.55±0.09	<0.001	1.08±0.29	0.395	0.82±0.15	0.154	0.16±0.03	<0.001
CPT-2	1±0.04	0.63±0.06	<0.001	0.67±0.10	<0.001	0.66±0.06	<0.001	0.67±0.05	<0.001
DGAT-1	1±0.04	1.20±0.12	0.071	0.58±0.18	0.003	0.60±0.04	<0.001	0.87±0.12	0.14
PGC-1α	1±0.09	0.52±0.06	<0.001	0.59±0.18	<0.005	0.94±0.18	0.395	1.34±0.31	0.17
UCP2	1±0.08	0.51±0.08	<0.001	0.39±0.08	<0.001	0.80±0.09	0.055	1.53±0.79	0.276
UCP3	1±0.06	0.75±0.09	0.020	0.50±0.11	<0.001	0.74±0.14	0.037	2.10±0.49	0.038
Nox1	1±0.21	3.31±0.61	0.006	4.87±1.82	0.026	0.90±0.19	0.378	1.17±0.42	0.367
Nox4	1±0.21	5.25±2.22	0.047	0.72±0.10	0.093	1.17±0.12	0.199	1.17±0.14	0.206

P values are versus untreated control. Ang II, angiotensin II; Hyd, hydralazine; Los, losartan; and NE, norepinephrine. Other abbreviations were same as Table 1.

semiquantitative measurements showed that the DHE-stained area was significantly greater after angiotensin II infusion (control 100±37%, $n=5$, versus angiotensin II 342±125%, $n=5$; $P<0.05$). In the heart of angiotensin II-infused rats, some myocardial cells that had increased superoxide staining were found to be positive for lipid deposition (lower magnification in Fig. 3A, B, and higher magnification in Fig. 3C–D). Similarly, some vascular wall and perivascular cells with increased superoxide staining were found to contain lipid deposits (Fig. 3G–J).

3.5. Regulation of genes related to lipid metabolism

Next, we examined the expression of lipid metabolism-related genes after infusion of the pressor agents (Table 2). mRNA expression of PPAR-α, PPAR-γ, SREBP-1c, FAS, and HMG-CoAR was found to be increased in the heart of rats that received angiotensin II infusion. Of the genes tested, mRNA expression of PPAR-α and PPAR-γ was also increased in the heart of the norepinephrine-infused rat. The expression of PGC-1α, UCP2 and UCP3 was decreased after angiotensin II infusion, but not after norepinephrine infusion. The angiotensin II-induced regulation of these genes (PPAR-α, PPAR-γ, SREBP-1c, FAS, HMG-CoAR, PGC-1α, UCP2, and UCP3) was suppressed by losartan, but not by hydralazine. On the other hand, mRNA expression of CPT-1 and CPT-2 was downregulated by angiotensin II. We found that the angiotensin II-induced CPT-1 downregulation was suppressed by depressor agents, and that norepinephrine also downregulated CPT-1 mRNA expression; therefore, the angiotensin II-induced CPT-1 mRNA downregulation might be induced by hypertension per se. Angiotensin II increased the mRNA expression of two components of NAD(P)H oxidase, Nox1 and Nox4.

Angiotensin II did not alter the protein expression of AMPKα; however, it increased the levels of phosphorylated AMPKα, and this increase was inhibited by either depressor agent (Fig. 4). Protein expression of matured SREBP-1 was increased by angiotensin II, and this increase was suppressed by losartan, but not by hydralazine.

We also examined the expression of several other lipid metabolism-related proteins. In the heart of control ($n=4$) and angiotensin II-

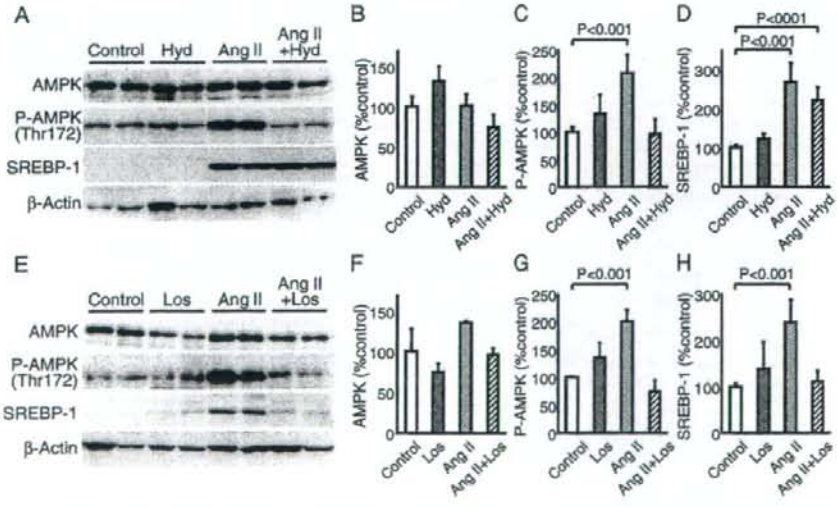

Fig. 4. Western blot analysis of AMP-activated protein kinase (AMPK), phosphorylated (activated) form of AMPKα (P-AMPK), and SREPB-1. A, E. Representative blots. B–D, F–H. Summary of data from 4–6 experiments in each group. Abbreviations are same as Table 1.

Please cite this article as: Hongo, M., et al., Administration of angiotensin II, but not catecholamines, induces accumulation of lipids in the rat heart, Eur. J. Pharmacol. (2009), doi:10.1016/j.ejphar.2008.12.006

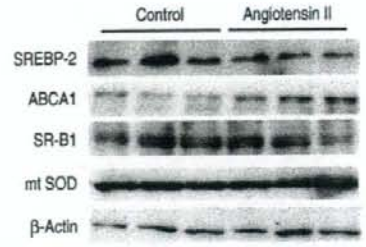

Fig. 5. Western blot analysis of proteins related to lipid metabolism. Shown are the results of the expression in the heart of control and angiotensin II-infused rats of the following proteins: Sterol regulatory element-binding protein (SREBP)-2, ATP-binding cassette transporter subfamily A-1 (ABCA1), scavenger receptor class B type 1 (SR-B1), mitochondrial superoxide dismutase (mt SOD).

infused ($n=4$) rats, the expression of these proteins was, respectively (% control): SREBP-2: 100±17 versus 78±14 (P=NS); ABCA1: 100±10 versus 172±7 ($P<0.001$); SR-B1: 100±17 versus 127±18 (P=NS); mit SOD: 100±5 versus 110±18 (P=NS) (Fig. 5).

4. Discussion

In the present study, we showed that administration of angiotensin II, but not catecholamines, caused accumulation of lipids in myocardial, vascular wall, and perivascular cells in the rat heart. Such angiotensin II-induced lipid deposition, as well as the increases in tissue triglyceride content in the heart, was suppressed completely by losartan, but only partially by hydralazine. These findings collectively indicate that the accumulation of intracardiac lipids induced by angiotensin II was, at least in part, independent of the pressor properties of angiotensin II.

Intracardiac lipid accumulation, which is sometimes designated 'cardiac steatosis' (McGavock et al., 2007), is known to occur in humans in certain diseased conditions, such as diabetes and heart failure (McGavock et al., 2007, Sharma et al., 2004). By means of genetic engineering, several animal models showing an amount of intracardiac lipids have been generated; these models include mice with cardiac-specific overexpression of acyl CoA synthase (Lee et al., 2004), fatty acid transport protein 1(Chiu et al., 2005), and PPAR-α (Finck et al., 2003), and mice with cardiac-restricted deletion of PPAR-delta (Cheng et al., 2004). The observation that accumulation of excessive fatty acids aggravates, whereas reduction of cardiac lipid content ameliorates, the structural and functional damage in these models supports the notion that accumulation of excessive lipid may indeed be cardiotoxic. In our previous studies, we found that administration of angiotensin II, but not catecholamines, caused marked accumulation of neutral lipids in the kidney (Ishizaka et al., 2006, Saito et al., 2005), leading us to investigate whether these two pressor agents affect cardiac lipid content differently in the current study.

What would be the mechanism underlying angiotensin II-induced intracardiac lipid deposition? We found that angiotensin II upregulated the expression of SREBP-1c, FAS, and HMG-CoAR, and downregulated that of UCP2, and UCP3; in addition, the pattern of regulation paralleled intracardiac lipid accumulation. It has been reported that angiotensin II upregulates the expression of SREBP-1c and FAS, resulting in increased lipogenesis in adipocytes in vitro (Jones et al., 1997, Kim et al., 2001). In addition, although the physiological functions of UCP2 and UCP3 are not well-established, downregulation of these new UCPs may augment the production of reactive oxygen species and decrease the catalysis of transported fatty acids (Affourtit et al., 2007). We also found that angiotensin II upregulated PPAR-α mRNA expression. Overexpression of PPAR-α in the heart may also cause lipotoxic cardiomyopathy (Finck et al., 2003, Vikramadithyan et al., 2005), suggesting that PPAR-α upregulation might be an underlying mechanism linking angiotensin II administration and cardiac lipid deposition.

Several previous studies have shown that PPAR-α activator may ameliorate myocardial damage induced by angiotensin II (Fujita et al., 2008, Ichihara et al., 2006). In the current study, we also found that PPAR-α expression was increased by norepinephrine infusion, which did not cause apparent cardiac lipid accumulation, indicating that upregulation of cardiac PPAR-α may not solely account for lipid accumulation in the heart. Whether or not PPAR-α activator acts to enhance or to suppress angiotensin II-induced lipid accumulation in the heart should be examined in future studies.

Activation of AMPK may result in the phosphorylation of acetyl CoA carboxylase, followed by the reduction of malonyl CoA and the subsequent activation and upregulation of CPT-1, leading to the stimulation of fatty acid oxidation (Affourtit et al., 2007). In the current study, we found that angiotensin II activated cardiac AMPK; however, it downregulated CPT-1 mRNA expression. Tian et al. (2001) have recently reported that pressure overload-induced cardiac hypertrophy causes a significant increase in AMPK activity in the heart that is, unexpectedly, accompanied by a downregulation of CPT-1 expression. They presumed that, unlike short-term activation, prolonged activation of AMPK might result in a downregulation of the enzymes that would be critical to fatty acid oxidation. With regard to this, it may be of note that, in the current study, both AMPK activation and CPT-1 downregulation by angiotensin II were suppressed not only by losartan, but also by hydralazine, and that CPT-1 mRNA downregulation was also induced by norepinephrine-induced hypertension, suggesting that these events were induced not in an angiotensin II-specific manner, but rather by hypertension itself.

It has been reported that UCP2 may reduce the generation of ROS, and conversely, downregulation of uncoupling proteins may increase the generation of ROS (Arsenijevic et al., 2000). On the other hand, enhanced oxidative stress or increased amounts of ROS may activate or upregulate SREBP-1 and FAS (Furuta et al., 2008, Gharavi et al., 2006). In addition, CuZn-SOD deficiency has been reported to increase lipid accumulation in the liver (Uchiyama et al., 2006). We found in our previous study (Saito et al., 2005) and the current one that superoxide is histologically co-localized with lipid deposition in the heart and kidney of angiotensin II-infused rats. Taken together, these findings may collectively suggest that angiotensin II-induced deposition of lipid in the heart may be evoked, at least in part, by enhanced oxidative stress (Fig. 5). This hypothesis should be examined in future studies (Fig. 6).

In conclusion, administration of angiotensin II to rats induced intracardiac lipid accumulation in regions where superoxide

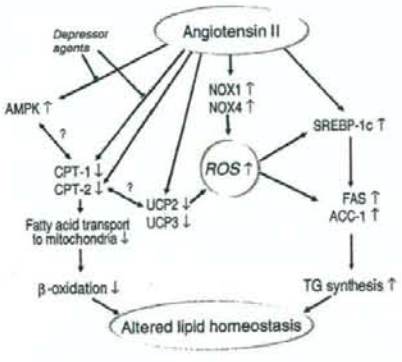

Fig. 6. Working hypothesis on angiotensin II-induced altered lipid homeostasis. Abbreviations are same as in Table 1. ROS indicates reactive oxygen species.

Please cite this article as: Hongo, M., et al., Administration of angiotensin II, but not catecholamines, induces accumulation of lipids in the rat heart, Eur. J. Pharmacol. (2009), doi:10.1016/j.ejphar.2008.12.006

production was found to be increased. The angiotensin II-induced accumulation of intracardiac lipids, in addition to regulation of the expression of several lipid metabolism-related genes (SREBP-1c, FAS, HMG-CoAR, PGC-1α, UCP2, and UCP3), events that were not mimicked by catecholamine infusion, were found to be dependent on the angiotensin AT_1 receptor. The physiological significance of angiotensin II-induced cardiac lipid accumulation and the role of enhanced oxidative stress on this phenomenon await further investigation.

Acknowledgements

This work was supported by Grants in Aid for Scientific Research from the Ministry of Education, Science, and Culture of Japan (Grant 19590937) and Grant from the Takeda Science Foundation, the Sankyo Foundation of Life Science, Okinaka Memorial Institute for Medical Research, and Daiwa Securities Health Foundation.

References

Affourtit, C., Crichton, P.G., Parker, N., Brand, M.D., 2007. Novel uncoupling proteins. Novartis Found. Symp. 287, 70–80 Discussion 80–91.

Aizawa, T., Ishizaka, N., Taguchi, J., Nagai, R., Mori, I., Tang, S.S., Ingelfinger, J.R., Ohno, M., 2000. Heme oxygenase-1 is upregulated in the kidney of angiotensin II-induced hypertensive rats: possible role in renoprotection. Hypertension 35, 800–806.

Arsenijevic, D., Onuma, H., Pecqueur, C., Raimbault, S., Manning, B.S., Miroux, B., Couplan, E., Alves-Guerra, M.C., Goubern, M., Surwit, R., Bouillaud, F., Richard, D., Collins, S., Ricquier, D., 2000. Disruption of the uncoupling protein-2 gene in mice reveals a role in immunity and reactive oxygen species production. Nat. Genet. 26, 435–439.

Cheng, L., Ding, G., Qin, Q., Huang, Y., Lewis, W., He, N., Evans, R.M., Schneider, M.D., Brako, F.A., Xiao, Y., Chen, Y.E., Yang, Q., 2004. Cardiomyocyte-restricted peroxisome proliferator-activated receptor-delta deletion perturbs myocardial fatty acid oxidation and leads to cardiomyopathy. Nat. Med. 10, 1245–1250.

Chiu, H.C., Kovacs, A., Blanton, R.M., Han, X., Courtois, M., Weinheimer, C.J., Yamada, K.A., Brunet, S., Xu, H., Nerbonne, J.M., Welch, M.J., Fettig, N.M., Sharp, T.L., Sambandam, N., Olson, K.M., Ory, D.S., Schaffer, J.E., 2005. Transgenic expression of fatty acid transport protein 1 in the heart causes lipotoxic cardiomyopathy. Circ. Res. 96, 225–233.

Finck, B.N., Han, X., Courtois, M., Aimond, F., Nerbonne, J.M., Kovacs, A., Gross, R.W., Kelly, D.P., 2003. A critical role for PPARalpha-mediated lipotoxicity in the pathogenesis of diabetic cardiomyopathy: modulation by dietary fat content. Proc. Natl. Acad. Sci. U. S. A. 100, 1226–1231.

Fujita, K., Maeda, N., Sonoda, M., Ohashi, K., Hibuse, T., Nishizawa, H., Nishida, M., Hiuge, A., Kurata, A., Kihara, S., Shimomura, I., Funahashi, T., 2008. Adiponectin protects against angiotensin II-induced cardiac fibrosis through activation of PPAR-alpha. Arterioscler. Thromb. Vasc. Biol. 28, 863–870.

Furuta, E., Pai, S.K., Zhan, R., Bandyopadhyay, S., Watabe, M., Mo, Y.Y., Hirota, S., Hosobe, S., Tsukada, T., Miura, K., Kamada, S., Saito, K., Iiizumi, M., Liu, W., Ericsson, J., Watabe, K., 2008. Fatty acid synthase gene is up-regulated by hypoxia via activation of Akt and sterol regulatory element binding protein-1. Cancer Res. 68, 1003–1011.

Gharavi, N.M., Baker, N.A., Mouillesseaux, K.P., Yeung, W., Honda, H.M., Hsieh, X., Yeh, M., Smart, E.J., Berliner, J.A., 2006. Role of endothelial nitric oxide synthase in the regulation of SREBP activation by oxidized phospholipids. Circ. Res. 98, 768–776.

Horiuchi, M., Yoshida, H., Kobayashi, K., Kuriwaki, K., Yoshimine, K., Tomomura, M., Koizumi, T., Nikaido, H., Hayakawa, J., Kuwajima, M., et al., 1993. Cardiac hypertrophy in juvenile visceral steatosis (jvs) mice with systemic carnitine deficiency. FEBS Lett. 326, 267–271.

Ichihara, S., Obata, K., Yamada, Y., Nagata, K., Noda, A., Ichihara, G., Yamada, A., Kato, T., Izawa, H., Murohara, T., Yokota, M., 2006. Attenuation of cardiac dysfunction by a PPAR-alpha agonist is associated with down-regulation of redox-regulated transcription factors. J. Mol. Cell. Cardiol. 41, 318–329.

Ishizaka, N., de Leon, H., Laursen, J.B., Fukui, T., Wilcox, J.N., De Keulenaer, G., Griendling, K.K., Alexander, R.W., 1997. Angiotensin II-induced hypertension increases heme oxygenase-1 expression in rat aorta. Circulation 96, 1923–1929.

Ishizaka, N., Aizawa, T., Yamazaki, I., Usui, S., Mori, I., Kurokawa, K., Tang, S.S., Ingelfinger, J.R., Ohno, M., Nagai, R., 2002. Abnormal iron deposition in renal cells in the rat with chronic angiotensin II administration. Lab. Invest. 82, 87–96.

Ishizaka, N., Matsuzaki, G., Saito, K., Noiri, E., Mori, I., Nagai, R., 2006. Expression and localization of PDGF-B, PDGF-D, and PDGF receptor in the kidney of angiotensin II-infused rat. Lab. Invest. 86, 1285–1292.

Jones, B.H., Standridge, M.K., Moustaid, N., 1997. Angiotensin II increases lipogenesis in 3T3-L1 and human adipose cells. Endocrinology 138, 1512–1519.

Kim, S., Dugail, I., Standridge, M., Claycombe, K., Chun, J., Moustaid-Moussa, N., 2001. Angiotensin II-responsive element is the insulin-responsive element in the adipocyte fatty acid synthase gene: role of adipocyte determination and differentiation factor 1/sterol-regulatory-element-binding protein 1c. Biochem. J. 357, 899–904.

Lee, Y., Naseem, R.H., Duplomb, L., Park, B.H., Garry, D.J., Richardson, J.A., Schaffer, J.E., Unger, R.H., 2004. Hyperleptinemia prevents lipotoxic cardiomyopathy in acyl CoA synthase transgenic mice. Proc. Natl. Acad. Sci. U. S. A. 101, 13624–13629.

McGavock, J.M., Lingvay, I., Zib, I., Tillery, T., Salas, N., Unger, R., Levine, B.D., Raskin, P., Victor, R.G., Szczepaniak, L.S., 2007. Cardiac steatosis in diabetes mellitus: a 1H-magnetic resonance spectroscopy study. Circulation 116, 1170–1175.

Saito, K., Ishizaka, N., Aizawa, T., Sata, M., Iso, O.N., Noiri, E., Ohno, M., Nagai, R., 2004. Role of aberrant iron homeostasis in the upregulation of transforming growth factor-beta1 in the kidney of angiotensin II-induced hypertensive rats. Hypertens. Res. 27, 599–607.

Saito, K., Ishizaka, N., Hara, M., Matsuzaki, G., Sata, M., Mori, I., Ohno, M., Nagai, R., 2005. Lipid accumulation and transforming growth factor-beta upregulation in the kidneys of rats administered angiotensin II. Hypertension 46, 1180–1185.

Schaffer, J.E., 2003. Lipotoxicity: when tissues overeat. Curr. Opin. Lipidol. 14, 281–287.

Sharma, S., Adrogue, J.V., Golfman, L., Uray, I., Lemm, J., Youker, K., Noon, G.P., Frazier, O.H., Taegtmeyer, H., 2004. Intramyocardial lipid accumulation in the failing human heart resembles the lipotoxic rat heart. Faseb. J. 18, 1692–1700.

Tian, R., Musi, N., D'Agostino, J., Hirshman, M.F., Goodyear, L.J., 2001. Increased adenosine monophosphate-activated protein kinase activity in rat hearts with pressure-overload hypertrophy. Circulation 104, 1664–1669.

Uchiyama, S., Shimizu, T., Shirasawa, T., 2006. CuZn-SOD deficiency causes ApoB degradation and induces hepatic lipid accumulation by impaired lipoprotein secretion in mice. J. Biol. Chem. 281, 31713–31719.

Unger, R.H., 2002. Lipotoxic diseases. Annu. Rev. Med. 53, 319–336.

Vikramadithyan, R.K., Hirata, K., Yagyu, H., Hu, Y., Augustus, A., Homma, S., Goldberg, I.J., 2005. Peroxisome proliferator-activated receptor agonists modulate heart function in transgenic mice with lipotoxic cardiomyopathy. J. Pharmacol. Exp. Ther. 313, 586–593.

Zhou, Y.T., Grayburn, P., Karim, A., Shimabukuro, M., Higa, M., Baetens, D., Orci, L., Unger, R.H., 2000. Lipotoxic heart disease in obese rats: implications for human obesity. Proc. Natl. Acad. Sci. U. S. A. 97, 1784–1789.

Please cite this article as: Hongo, M., et al., Administration of angiotensin II, but not catecholamines, induces accumulation of lipids in the rat heart. Eur. J. Pharmacol. (2009), doi:10.1016/j.ejphar.2008.12.006

皮膚病診療
Vol.30, No.12
<別　刷>

Kaposi肉腫——最新の知見

上田　啓次

㈱協和企画

皮膚病診療：30(12)；1344～1348, 2008

展望 I

Kaposi肉腫——最新の知見——

上田　啓次*

Key words
Kaposi肉腫，KSHV，k1，v-gpcr

はじめに

1872年にMoritz Kaposiが初めて5例の進行型(aggressive)Kaposi肉腫(Kaposi's sarcoma，KS)を報告してからすでに140年足らずの年月が経過した[1]．この間，その起源細胞や病因に関して多くの研究が展開されてきた．KSはアフリカ中部域の若年男性にみられる進行型KSが多いとされるアフリカ型風土病KS(African endemic KS)，東ヨーロッパや地中海沿岸地域の高齢者を中心として発生する古典的KS(Classic KS)，アメリカ合衆国西部に端を発したヒト免疫不全症ウイルス(human immuno-deficiency virus1および2，HIV-1および-2)感染によりひきおされる，後天性免疫不全症候群(acquired immuno-deficiency syndrome，AIDS)の流行に伴ってその発生が注目された男性同性愛者のAIDS随伴症として発生するAIDS-KS，さらに医原性KS(iatrogenic KS)，HIV陰性男性同性愛者に発生するKS(HIV-negative gay men with KS)に大きく分類される(**表1**)[2]．KSはこのように風土病的要素が強いこと，免疫不全に伴って発症する可能性が高いことなどから，感染因子がその病因であることが古くから指摘されていた．またその病因については基本的にHIV蔓延地域と重なることや，AIDSが基礎疾患に多いことからHIVが病因因子であるという予測のもと多くの研究が展開されてきた．しかしながら，古典的KSの多くやHIV陰性男性同性愛者に発生するKSを考慮すると，別の病因因子があると考えざるをえないことから，1980年代後半から1990年代前半にかけて病因因子の同定が精力的に行われてきた．

表1　Kaposi肉腫の分類

AIDS-KS
古典的KS
医原性KS
アフリカ風土病的KS
男性同性愛者HIV陰性KS

そして1994年，コロンビア大学のChang，Mooreのグループによりその断片が同定された．彼らはrepresentational difference analysis(RDA)を駆使して核酸断片のクローニングに成功し，その配列がγヘルペスウイルス属に属するherpesvirus saimiri(HVS)や，Epstein-Barr virus(EBV)に相同性を示したことから，KSに密接に関連しヒトに感染する8番目のヘルペスウイルスで第2のγヘルペスウイルス(Kaposi's sarcoma-associated herpesvirus[KSHV]もしくはhuman herpesvirus 8[HHV-8]，本稿では通称名であるKSHVと表記する)として認識されるに至った[3~9]．

本稿ではKSの原因ウイルスであるKSHVのウイルス学的側面と，本ウイルスによるKS発症機構に関する最新の知見を解説したい．

Ⅰ．KSHVのゲノム構造と遺伝子

前述のごとくKSHVはγヘルペスウイルスの1つで，ゲノムは約140kbの固有領域と約30～50kbの

* Ueda, Keiji(教授)　浜松医科大学医学部感染症学感染機構解析分野(〒431-3192 浜松市東区半田山1－20－1)

末端反復配列(terminal repeats, TR)からなる[10]. 80～90の遺伝子は約140kbの固有領域のみにあると考えられ, TRには遺伝子が存在するとの報告はいまのところない. ウイルス構造遺伝子はヘルペスウイルス間で相同性が高く, とくにEBVとの相同性はより高いと考えられる. 一方, KSHVに固有の遺伝子が数多く存在し, とくに宿主から略奪したと考えられるものが数多く存在する. これらの中には発癌性(oncogenic)もしくは発癌に関わる可能性がある遺伝子も多く存在する(**表2**)[11].

表2 KSHVがもつ宿主由来遺伝子

細胞増殖：	*v-cyclin*(ORF72) *v-GPCR*(ORF74) *v-IRF*(K9, K10s)
アポトーシス抑制：	*v-bcl2*(ORF16) *v-FLIP*(ORF71/K13) *v-IL6*(K2)
ケモカイン：	*v-MIP I*(K4) *v-MIP II*(K6) *v-MIP III*(K4.2)
細胞内シグナリング：	*v-NCAM*(K14)

Ⅱ. KSHVによるKS発症機構

γヘルペスウイルスはEBVで知られるように腫瘍あるいは腫瘍性疾患の発症に深く関わっているとされる. 動物界に蔓延しているγヘルペスウイルスも然りである(**表3**). 多発性骨髄腫, サルコイドーシス, 最近では原発性肺高血圧症にKSHVが起因しているとの報告があったが, 原段階ではこれらの疾患との関連は否定的であり, KSHVが関連する病態は主に3つと考えていいのではないかと思われる[12-16]. それらはKS, primary effusion lymphoma(PEL)およびmulticentric Castleman's disease(MCD)であり, これらの疾患では統計にもよるがほぼ100%検出される[2, 5, 17, 18]. PELとMCDはB細胞を起源とする腫瘍, あるいは腫瘍性の疾患であるが, KSを含めこれら3つの疾患はAIDSを基礎疾患としてもつことが多い. このことは確かにKSHVの病原性が免疫不全に伴って活性化することを示している.

1. KSHV感染系によるKS発生モデル

KSの起源細胞については, 病巣を構成する基本組織として血管様組織の増生と介在する紡錘形細胞(紡錘細胞, 紡錘体細胞, 紡錘型細胞)からなると考えられ, 病理学的にも複雑であると思われるが, KSHVによるKS発症機構の解析では, 歴史的背景から血管内皮細胞を感染標的細胞として用いた報告がいくつかある. KSHV感染によりこれらの細胞がKSに酷似して紡錘形化し, テロメラーゼ活性の上昇, 接触阻止能の喪失や接着非依存性増殖などを示す[19-24]. また感染細胞ではvascular endothelial growth factor(VEGF)とそのレセプターの発現亢進をもたらし, autocrine/paracrine的に増殖を補助すると考えられている. これらの知見はKSHVが確かに標的細胞に対して不死化やト

表3 種々のγヘルペスウイルスと関連疾患

ウイルス	宿主	関連腫瘍性疾患
Kaposi's sarcoma associated herpesvirus(KSHV)	ヒト	Kaposi肉腫(KS), primary effusion lymphoma(PEL), multicentric Castleman's disease(MCD)
Epstein-Barr virus(EBV)	ヒト	バーキットリンパ腫, Hodgkin病, 移植後リンパ球増殖症, 鼻咽頭腫
Herpesvirus saimiri(HVS)	新世界ザル	T細胞腫, リンパ肉腫
Retroperitoneal fibrosis herpesvirus(RPHV)	旧世界ザル	後腹膜線維腫
Murine herpesvirus 68(MHV68)	マウス	リンパ球増殖症

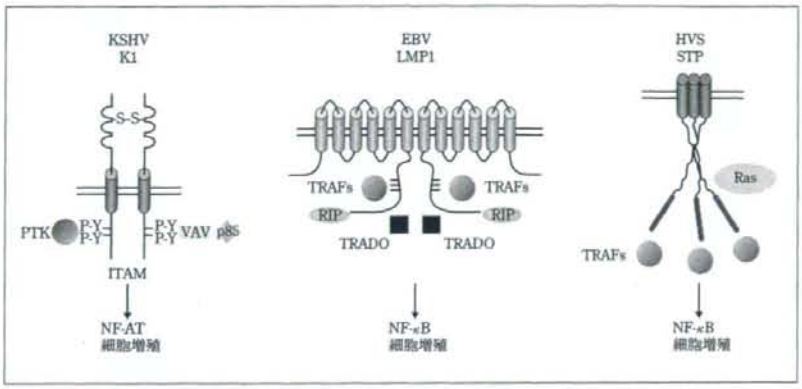

図1　KSHV癌遺伝子*k1*とその類似遺伝子(文献6より改変)

ランスフォーメーション能を有することを示すものである.

2. KS発生に関わるウイルス遺伝子

それでは多くのウイルス遺伝子のうちどれが前述の現象を惹起しKS発生と密接に関わっているのであろうか[25, 26]? KSHVに関連する3つの腫瘍あるいは腫瘍様疾患においては, KSHVの感染形態がヘルペスウイルスの特徴とされる潜伏感染であることから, 潜伏感染状態で発現している遺伝子が注目された. KSHV潜伏感染で発現しているウイルス遺伝子は, 一領域4遺伝子(*lana*, *v-cyc*, *v-flip*, *k12*[*kaposin*])のみである(宿主interferon regulatory factor[IRF]相同遺伝子の1つである*k10.1*[*lana2*と呼ぶ研究者もいる]も発現しているとの報告もある)が, これらの遺伝子のトランスフォーメーション活性はほとんどなく(私信), これらの遺伝子によりKSが直接誘導されるということは否定的と考えている. 現在, KSHV遺伝子の中で不死化/トランスフォーメーション活性を有すると考えられているのは*k1*と*orf74*(*v-gpcr*)であり, これらは溶解複製時に発現する遺伝子である. 潜伏感染関連遺伝子の機能としてはLANAによるp53やpRbの不活化や[27, 28]Wntシグナルの恒常的活性化[29], v-CYCによるcyclin dependent kinase inhibitor(CDKI)の機能抑制や紡錘糸機能異常による多核細胞の形成など, 直接的に発癌に関わっている側面ももっているが[30, 31], むしろ, LANAはウイルスゲノムの複製・分配・維持[32], v-CYCはG1からS期への細胞周期亢進[30], v-FLIPはCa動員によるアポトーシスの抑制[33], KAPOSINはMAPK(mitogen activated protein kinase)を活性化する[34]ことにより*k1*や*v-gpcr*によって不死化/トランスフォーメーションされた細胞の形質維持に関わっていると考えるほうが妥当ではないかと考えている(私信).

a. *k1*遺伝子の発癌機能

*k1*遺伝子はKSHVゲノム固有領域の最端に位置する289アミノ酸からなる膜蛋白をコードし, 溶解複製時の比較的遅い時期に発現する遺伝子である. Jungらの解析によりK1が強いトランスフォーメーション活性をもつことが示されている[35-37]. 本遺伝子の機能の中枢はimmunoreceptor tyrosine-based activation motif(ITAM, [D/E]X$_7$[D/E]X$_2$YX$_2$LX$_7$YX$_2$[L/I])にあり, このモチーフを介してphosphotyrosine kinases(PTKs)によるリン酸化がおこるとVav, Syk, PI3Kなどと相互作用し, さらに下流へシグナルを伝えるものと考えられている. N末は細胞外ドメインを形成してなんらかのリガンドに特異的に結合することも予想されるが, 本ドメインはKSHVクローン間での変異が多く, 特定のリガンドの存在は考えにくい. このことはKSHVのクローンにより発癌性が異なることも意味しているが, ITAMをもつC末は逆に保存性が高くむしろ恒常的にPTKsによるリン酸化を受け活性化し, 最終的にはNF-ATを介した遺伝子発現誘導による増殖制御に関わっているものと考えられている.

類縁γヘルペスウイルスであるHVSではsaimiri transformation proteins(*stp*), EBVでは*LMP1*(ただし, *LMP1*はゲノム上の位置的な相同遺伝子で

ITAMを有する遺伝子としては*LMP2A*が存在し，また*LMP2A*の位置的相同遺伝子はKSHVでは*k15*とされる)が存在し，NF-κBシグナリングを活性化することで発癌性に関わっていると考えられている(図1)[38]．*k1*遺伝子のKS形成に関する機能はよくわかっていないが，トランスジェニックマウスにおける発癌能を考えると十分関わっているものと想定される[35]．

b．*v-gpcr*の発癌機能　KS形成に関してもっとも重要な働きをしていると考えられているKSHV遺伝子は*v-gpcr*であり，*in vitro*，*in vivo*においてその潜在的腫瘍系性能が示された[39-49]．v-GPCRはCXC-Rタイプのケモカインレセプターとして機能し，IL-8/CXCL8，Gro-α/CXCL1のレセプターとして機能し，またVEGFとそのレセプターVEGFレセプター-2/kinase insert domain-containing receptor(VEGF-R2/KDR)を発現誘導し，さらにテロメラーゼ活性を高めることで*in vitro*で血管内皮細胞を不死化/トランスフォーメーションする活性をもつ[44, 50]．Inducible protein-10(IP-10/CXCL10)やCXCL12/SDF1はv-GPCRに対して抑制的に作用するもののKSの周囲環境が種々のケモカイン，サイトカインに溢れていて，種々の宿主リガンドに反応可能なことはKS形成に重要な意味をもっている[51]．

v-GPCRは，PI3K-AKT/protein kinase B(PKB)経路を刺激しアポトーシスを抑制する．AKT/PKB経路の活性化はG proteinsβγに依存しているとされるが，前述のごとく，KSHV感染によるVEGF-VEGF-R2/KDRの活性化によりautocrine/paracrine的に活性化することでも達成されていると考えられている[43]．このようなv-GPCRやVEGF-R2/KDRを介したシグナルはp38，Ras-extracellular signal-regulated kinase(ERK)，Rac1-Jun N-terminal kinase(JNK)等を通じてAP-1，NF-κB，hypoxia-inducible factor-1α(HIF-1α)の活性化と標的遺伝子の発現誘導に関わるものと考えられている[51, 52]．

c．KS形成に関わるその他のKSHV遺伝子　KSHVには癌遺伝子としての活性をもつとされる前述の2つの遺伝子に加え，補助的に発癌に関わる遺伝子がほかにも存在する．*v-bcl-2*(*orf-16*)[53, 54]，*v-NCAM*(*k14*)[55]，*v-IL-6*(*k2*)[35, 56, 57]，*v-MIPs*(*k4*，*k6*)[56, 58, 59]，*v-IRFs*(*k9*，*k10*，*k11*)[60]などは宿主免疫機能を攪乱し，増殖シグナルを送りつつ細胞死を回避するうえで極めて重要な機能を担っていると想定される[61]．もちろん潜伏感染で発現している遺伝子も潜伏感染を維持し，発癌母地を樹立している意味で病態形成に重要な役割を果たしていると考えられる．

Ⅲ．Kaposi肉腫の遺伝子発現プロファイル

近年のDNA array解析の発展により，腫瘍を含めた組織特異的な遺伝子発現プロファイルの解析が容易になった．KSHVが関連するPELやKSでの解析もいくつか報告されている．われわれが学生時代には教科書的にはKSの起源細胞は血管内皮細胞であろうと書かれていた記憶があるが，KSそのものの病巣はかなり複雑で一様な組織ではない可能性がある．このような状況下でKS組織を用いてなされた遺伝子発現プロファイル解析では，KS組織におけるそれは血管内皮細胞よりリンパ管内皮に近いことを示し，一定のインパクトを与えた[62]．*v-gpcr*を導入したマウスモデルではウイルス本来の発現制御機構に依存していないため，KS様の病巣が確かに形成されるとしても実際の患者KSとは異なる可能性があり，今後こうした個体モデルでより詳細な検討が必要と思われる．

おわりに

Kaposi肉腫原因因子KSHVが発見されて100年余，凄まじい勢いでその生物学，本ウイルスによるKSやPELの病態発症機構について研究がなされてきた．DNAウイルスによる腫瘍発生機構はSV40，アデノウイルス，パピローマウイルス，EBVなどを用いた解析により多くの知見がある．しかしながら，これらのウイルス感染患者の多くが癌を発症するわけではなく，それはむしろごく一部分であり，ウイルス感染と発癌との間には未解明のblack boxが存在する．KSHVでは潜伏感染状態は確かに発癌母地を形成しているという意味で重要な感染形態であるが，潜在的発癌活性をもつ遺伝

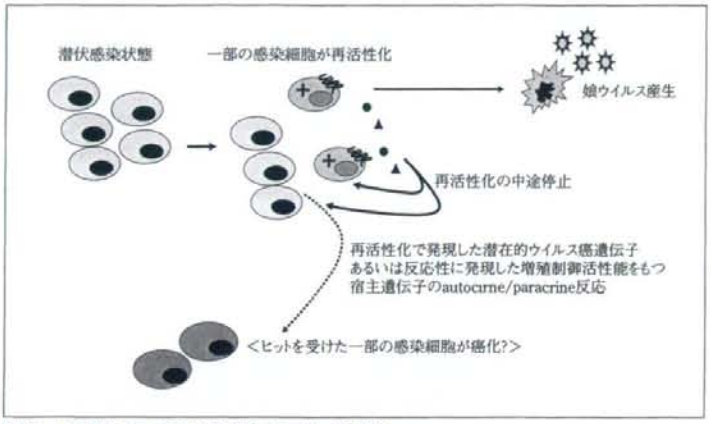

図2　KSHVによるKS発生モデル(私信)

子は溶解複製時に発現する遺伝子である．発癌に関わるとされる*k1*や*v-gpcr*を含め発癌に関わるウイルス遺伝子ががどのような局面で発現し，発癌に至らしめるのか詳細な解析が待たれる(**図2**)．

<文　献>

1) Kaposi, M. : Arch Dermatol Syphilol **4** : 265, 1872
2) Boshoff, C. , Weiss, R.A. : Adv Cancer Res **75** : 57, 1998
3) Chang, Y. et al. : Science **266** : 1865, 1994
4) Sarid, R. et al. : Adv Virus Res **52** : 139, 1999
5) Antman, K., Chang, Y. : N Engl J Med **342** : 1027, 2000
6) Offermann, M.K. : Trends Microbiol **4** : 383, 1996
7) Schulz, T.F. : J Gen Virol **79** : 1573, 1998
8) Sturzl, M. et al. : Adv Cancer Res **81** : 125, 2001
9) Boshoff, C., Chang, Y. : Annu Rev Med **52** : 453, 2001
10) Russo, J.J. et al. : Proc Natl Acad Sci USA **93** : 14862, 1996
11) Damania, B., Jung, J.U. : Adv Cancer Res **80** : 51, 2001
12) Brander, C. et al. : Blood **100** : 698, 2002
13) Knoell, K.A. et al. : Arch Dermatol **141** : 909, 2005
14) Fredricks, D.N. et al. : Clin Infect Dis **34** : 559, 2002
15) Rimar, D. et al. : Isr Med Assoc J **8** : 489, 2006
16) Bendayan, D. et al. : Respiration **75** : 155, 2008
17) Hengge, U.R. et al. : Lancet Infect Dis **2** : 344, 2002
18) Hengge, U.R. et al. : Lancet Infect Dis **2** : 281, 2002
19) Ciufo, D.M. et al. : J Virol **75** : 5614, 2001
20) Moses, A.V. et al. : J Virol **73** : 6892, 1999
21) Flore, O. et al. : Nature **394** : 588, 1998
22) Cerimele, F. et al. : J Virol **75** : 2435, 2001
23) Cannon, J.S. et al. : J Virol **74** : 10187, 2000
24) Boshoff, C. et al. : Nat Med **1** : 1274, 1995
25) Damania, B. : Nat Rev Microbiol **2** : 656, 2004
26) Ensoli, B. et al. : Adv Cancer Res **81** : 161, 2001
27) Friborg, J., Jr. et al. : Nature **402** : 889, 1999
28) Radkov, S.A. et al. : Nat Med **6** : 1121, 2000
29) Liu, J. et al. : J Virol **81** : 4722, 2007
30) Laman, H. et al. : Mol Cell Biol **21** : 624, 2001
31) Verschuren, E.W et al. : Cancer Cell **2** : 229, 2002
32) Ballestas, M.E. et al. : Science **284** : 641, 1999
33) Thome, M. et al. : Nature **386** : 517, 1997
34) McCormick, C., Ganem, D. : Science **307** : 739, 2005
35) Prakash, O. et al. : J Natl Cancer Inst **94** : 926, 2002
36) Lee, H. et al. : Mol Cell Biol **18** : 5219, 1998
37) Lee, H. et al. : Nat Med **4** : 435, 1998
38) Brinkmann, M.M., Schulz, T.F. : J Gen Virol **87** : 1047, 2006
39) Gershengorn, M.C. et al. : J Clin Invest **102** : 1469, 1998
40) Montaner, S. et al. : Cancer Res **61** : 2641, 2001
41) Nador, R.G. et al. : Virology **287** : 62, 2001
42) Schwarz, M., Murphy, P.M. : J Immunol **167** : 505, 2001
43) Bais, C. et al. : Cancer Cell **3** : 131, 2003
44) Montaner, S., et al. : Cancer Cell **3** : 23, 2003
45) Boshoff, C. : Nature **391** : 24, 1998
46) Rosenkilde, M.M. et al. : Oncogene **20** : 1582, 2001
47) Rosenkilde, M.M. et al. : J Biol Chem **274** : 956, 1999
48) Guo, H.G. et al. : J Virol **77** : 2631, 2003
49) Arvanitakis, L. et al. : Nature **385** : 347, 1997
50) Lane, B.R. et al. : J Virol **76** : 11570, 2002
51) Sodhi, A. et al. : Nat Rev Mol Cell Biol **5** : 998, 2004
52) Zhang, X. et al. : J Biol Chem **280** : 26216, 2005
53) Sarid, R. et al. : Nat Med **3** : 293-8, 1997
54) Cheng, E.H. et al. : Proc Natl Acad Sci U S A **94** : 690, 1997
55) Foster-Cuevas, M. et al. : J Virol **78** : 7667, 2004
56) Moore, P.S. et al. : Science **274** : 1739, 1996
57) Chatterjee, M. et al. : Science **298** : 1432, 2002
58) Boshoff, C. et al. : Science **278** : 290, 1997
59) Lalani, A.S. et al. : Immunol Today **21** : 100, 2000
60) Shin, Y.C. et al. : J Virol **80** : 2257-66, 2006
61) Murphy, P.M. : Nat Immunol **2** : 116-22, 2001
62) Hong, Y.K. et al. : Nat Genet **36** : 683-5, 2004